SELECTIVELY VENTILATED RING WING HYDROFOILS

Department of the Navy
Naval Ordnance Systems Command
Weapon Dynamics Division, Code ORD-035
Contract Nonr 220(54)

HYDRODYNAMICS LABORATORY
KÁRMÁN LABORATORY OF FLUID MECHANICS AND JET PROPULSION

CALIFORNIA INSTITUTE OF TECHNOLOGY

PASADENA, CALIFORNIA

Division of Engineering and Applied Science
California Institute of Technology
Pasadena, California

SELECTIVELY VENTILATED RING WING HYDROFOILS

Department of the Navy
Naval Ordnance Systems Command
Weapon Dynamics Division, Code ORD-035
Contract Nonr 220(54)

A. J. Acosta
and
R. B. Wade

Report No. E-138.2

August 1967

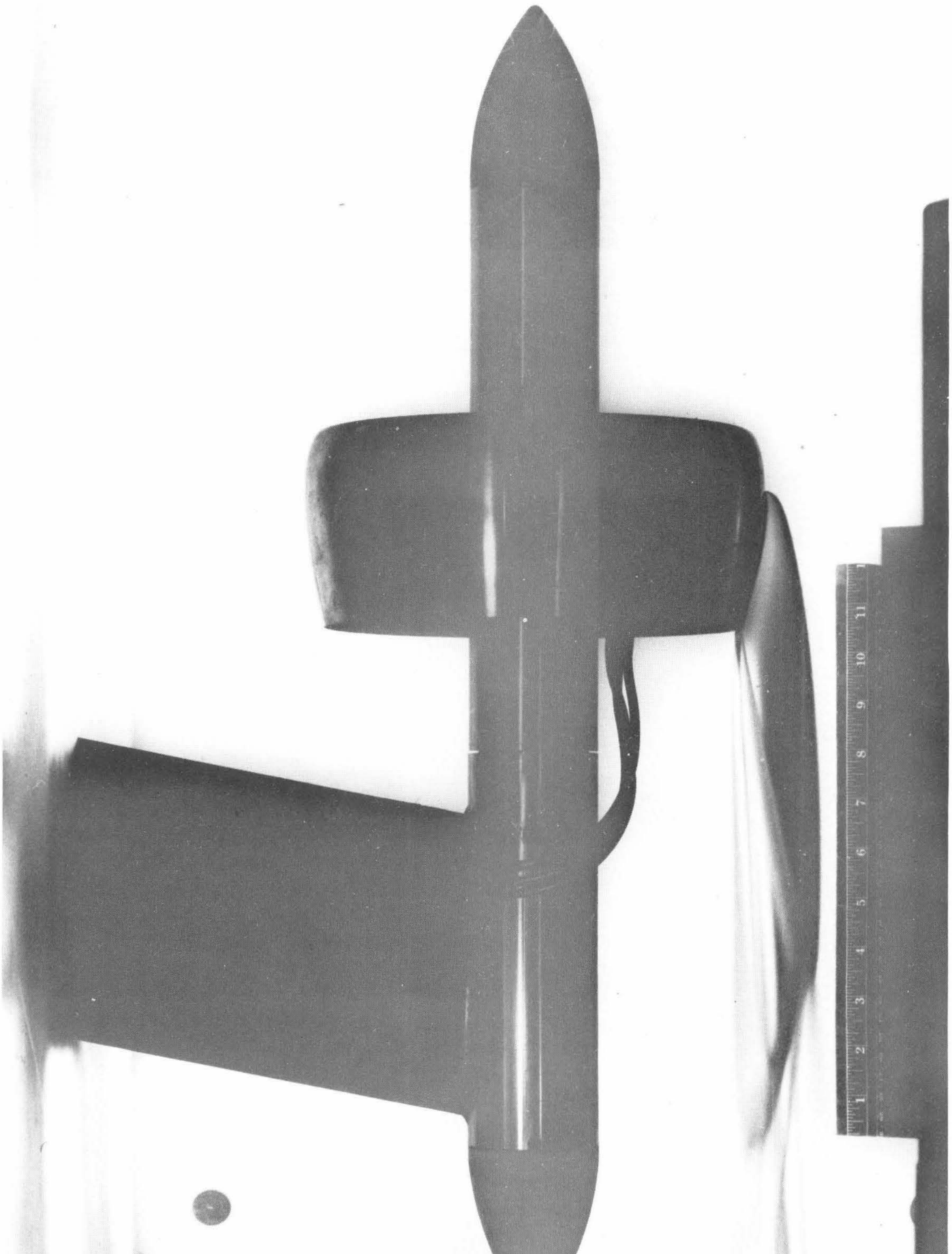
1 2 3 4 5 6 7 8 9 10 11

Division of Engineering and Applied Science
California Institute of Technology
Pasadena, California

FINAL REPORT

Contract Nonr 220(54)

SELECTIVELY VENTILATED RING WINGS

Abstract

Experiments were made on a ring wing having a chord-diameter ratio of one-half with a profile section consisting of a 10 percent Clark Y airfoil. Measurements were made of the force characteristics of this ring wing in fully wetted flow for several Reynolds numbers and angles of attack; in fully wetted flow these observations agreed with similar previous results on fully wetted ring wings. A portion of the circumference of the ring was also ventilated by the controlled injection of air to provide a cross-force. The magnitude of this cross-force varies with extent of ventilation and with the rate of injection of air. With less than approximately 11 percent of the trailing edge of the wing so ventilated, the cross-force corresponds to the wing in fully wetted flow having an angle of attack of nearly three degrees. Experiments were also made on the rapidity with which this cross-force could be built up at the start of injection or terminated after the ventilation had been established. The termination of the cross-force is very quick and amounts to a time approximately required for the flow to travel a distance of a few wing chords. The build-up process on the other hand is considerably slower, and it appears to be a dynamic one but the scaling laws for this phenomenon are not yet established.

Nomenclature

c - chord

C_D	-	drag coefficient; $D/\frac{1}{2}\rho V^2 \pi dc$
C_L	-	lift coefficient; $L/\frac{1}{2}\rho V^2 \pi dc$ (positive up)
C_M	-	moment coefficient; $M/\frac{1}{2}\rho V^2 d^2 c$ (positive nose up)
C_Q	-	air flow coefficient; $Q/\frac{\pi}{4} d^2 V$
d	-	diameter of ring wing
D	-	drag force
K	-	ventilation parameter; $(p_\infty - p_c)/\frac{\rho}{2} V^2$
L	-	lift force
M	-	moment about leading edge
p_c	-	pressure in cavity
p_∞	-	freestream pressure at elevation of cavity
Q	-	air volume flow rate at pressure p_∞
Re	-	Reynolds number, Vc/ν
V	-	freestream velocity
α	-	angle of attack to centerline of ring
ρ	-	liquid density
$\tau_{.7}$	-	time required to achieve 70 percent of steady lift force
$\tau_{.5}$	-	time required to achieve 50 percent of steady lift force
ν	-	kinematic viscosity

1. Introduction

The present work is a sequel to that of Reference 1 in which experiments were carried out on fully wetted and fully ventilated ring wings having conical sections. Preliminary experiments were also carried out in Reference 1 on the effect of selectively ventilating only a portion of a ring wing. It was found there that appreciable cross-forces normal to the oncoming flow could be developed by such selective ventilation and that the magnitude of these forces was clearly enough to

provide a force for a control function comparable to that of some existing underwater torpedos. The present work continues the study of selective ventilation but on a ring wing having a profile section more suitable for ventilation. This study together with that of Reference 1 stems from the work of Lang, Daybell and Smith (Ref. 2), in which selective ventilation on a series of two-dimensional hydrofoils was carried out in an attempt to develop control forces other than that of conventional movable surfaces. The present work is thus an extension of that of Reference 2 to wings of revolution. Like that of Reference 2, the magnitude of the steady forces caused by the ventilation process is of concern here, but in addition the time-behavior of the forces that are developed on the ring as the ventilation process is started and stopped is examined. The mutual influence between adjacent ventilating regions on the ring wing is also briefly investigated.

The suggestion of Smith that ventilation could be used to generate a possible control force is spelled out more specifically in a patent assigned to him (Ref. 3). However, other groups have been concerned with this same principle and although no engineering data have been published to our knowledge, the ventilation principle seems now to be applied to hydrofoil boat stabilization (Ref. 4) and has been considered for the control of underwater bodies (Ref. 5). The present study should then be helpful to other workers concerned with the development of ventilation as a control technique and it provides some quantitative data on the magnitude and speed of response of the effect.

The concept of using controlled injection of a non-condensible gas to change the external flow of an otherwise fully wetted body is in itself extremely simple. In two-dimensional flows the effect of such ventilation can be worked out fairly completely (Ref. 6) because in the steady state a ventilating flow closely resembles a free streamline flow, and well-known mathematical techniques are available for handling this type of problem in two-dimensional potential flow.

However, if surfaces of low aspect ratio or if lifting surfaces of revolution such as the ring wing are considered, then this type of analysis becomes exceedingly complex, and so far as is known there have been no theoretical attempts to treat the problem of selective ventilation with these configurations. Even so, practical problems arise in the application of the ventilation technique for which theory alone cannot provide the answer. These include the already mentioned dynamic process of the build-up and decay of the force when the ventilating supply is either commenced or terminated and other problems of application of the ventilation procedure to a hydrofoil in a real fluid flow.

One key to the successful application of this concept is found in the work of Lang (Ref. 2) in which it is pointed out that the ventilation will start at and take place entirely downstream of the gas injection point when the liquid flow over the profile shape is not separated. This is highlighted also in the experiments of Reference 1 where the ventilation was effected behind a conical ring wing. In fully wetted flow a conical ring which in profile shape is simply that of a flat plate inclined to the flow is usually separated at the leading edge. This separation bubble may reattach itself to the profile surface downstream of the leading edge if the Reynolds number is sufficiently high as was shown for the 12 degree included angle cone of Reference 1. Axisymmetric ventilating flows were easy to establish there although in order to produce a selectively ventilated flow on this ring, fences had to be mounted on the ring to prevent the ventilating gas from flashing around the circumference of the ring, thereby defeating the intent to ventilate only over a selected portion of the ring surface. Another essential consideration in using ventilation for a control force is in determining the response time. It may be recalled from aerodynamic experience that if an airfoil is given a sudden increase in angle of attack, half the subsequent change in lift occurs instantaneously and the steady state lift is achieved after the

time that it takes for the flow to travel a distance of about six chord lengths. In the present work it will be shown that ventilation termination is easily accomplished if the hydrofoil is normally unseparated. In fact the decay time for this process is just about that required for the freestream velocity to travel a few chord lengths. The build-up of the ventilating force, as we will see, is somewhat more complex but for successful operation to be obtained the injection process must again take place on a normally unseparated profile.

In the following paragraphs, the ring wing selected for experimentation will be described as will the associated instrumentation. Several different modifications were made to the ventilating gas supply system; they will be described chronologically as they occurred throughout the experimental program. To begin with, measurements of the forces in the steady ventilation condition will be discussed in which the effect of the pattern of the ventilating orifices will be treated and then we will pass on to a description and discussion of the transient measurements.

2. Experimental Apparatus

2.1 - Water Tunnel Facility

The present experiments, like those of Reference 1, were carried out in the Free Surface Water Tunnel of the Hydrodynamics Laboratory at the California Institute of Technology. This tunnel provides a flow ranging from about 2 to 25 feet per second in a working section approximately 20 inches square and 8 feet in length. Normally it has a free surface exposed to the atmosphere; the tunnel may be made into a closed working section by adding a rigid plate on the top surface. For the present work, however, the upper surface was left free. The range of velocities actually used in the present work was from 10 to 22 feet per second. The chord of the ring wing finally selected for use was 4 inches. As a result the maximum Reynolds number based on the chord length was only about

6×10^5, a value which is rather low for the present type of work. The turbulence level of the tunnel is by aerodynamic standards rather high. Though no precise measurements of this quantity have been made, it is estimated to be on the order of one percent.

2.2 - Experimental Model

To fit within the confines of the tunnel and yet provide forces sufficiently sensible for the readout equipment, the dimensions of the ring wing chosen for study are 4 inches chord and 8 inches diameter. The chord-diameter ratio of one-half is probably somewhat high for a conventional torpedo application and perhaps somewhat too low for a pump-jet application, yet with these proportions the three-dimensional effect is significant so that the results obtained should be representative.

The gist of the ventilation concept lies in changing the lift on a fully wetted profile to a much lower value by the injection of gas on the normal suction surface of the profile shape. Thus to provide the cross-force effect on an axisymmetric ring wing would require that the elements of the ring have a radially outward lift force. Such a lift force can be obtained either through angle of incidence to the oncoming flow or through camber, or both. The ultimate magnitude of the cross-force developed will of course then depend upon the magnitude of the original fully wetted radial force. Yet for the reasons mentioned above one cannot have too high a radial force coefficient or the profile shape will run the risk of separation and if the radial lift force is too low the effect of ventilation will be too small. As a choice between these extremes, the present wing was designed to have a radial force coefficient of approximately 0.5. For manufacturing and experimental convenience it was decided to make the inside of the ring cylindrical and parallel to the oncoming flow. The natural choice for a profile section would then be either one of the Walchner type or a Clark Y profile. A Clark Y profile of 10 percent thickness was finally chosen for this application; in a two-dimensional flow this section would produce a lift coefficient of

0.52 which seemed satisfactory for the present experiments although the pressure distribution is not the best one for the relatively low Reynolds numbers used. The ring is supported by two interior struts which are vertically oriented in the tunnel. The struts in turn are attached to a 2-1/4 inch diameter cylindrical hub. This hub is then clamped onto a centrally mounted strain gage sting balance, the same one described in Reference 1. Provision for supplying the ventilating gas, turning it off and on, and measuring the pressure of the subsequently formed ventilation cavity is made in the lower strut, the location of the ventilating holes. The coordinates of the Clark Y profile shape used for manufacture of the present ring are given in Table A-1 of the Appendix. Some of the details of the ring assembly and internal passages in the original model are shown in Figure A-1 of the Appendix.

As previously mentioned, the Reynolds number for this work is relatively low, being a maximum of 6×10^5, and for tests at lower speed the Reynolds number actually gets down to 3×10^5. It was found, as could be anticipated, that a laminar separation bubble existed near the leading portion of the profile and that this had a deleterious effect upon the selective ventilation scheme. A trip wire 0.01 inch in diameter was then installed one-quarter of an inch from the leading edge. The effect of the trip wire was to eliminate the presence of the separation bubble and satisfactory ventilation patterns could then be observed at all velocities.

2.3 - Ventilation Provisions

The ventilating gas used in all cases was regulated house air which had a maximum pressure of approximately 80 psig. The air supply was filtered and passed through a reducing valve to the model and model support assembly. The model and support assembly are shown schematically in the tunnel in Figure 1. For the first set of experiments provision was made to admit the air into a small plenum chamber placed within the profile of the ring. The details of this may be seen in Figure A-1. Provision was also

made to start and to stop this ventilating air by incorporating a pressure actuated shuttle valve within one of the struts supporting the ring, as can be seen in Figure A-1. Another orifice on the surface of the wing, downstream of the ventilating orifice, was provided so that the pressure within the cavity could be measured. The supply air, the control air and the air cavity pressure measurements were all brought through one of the struts and let out of the ring assembly through the model support assembly to the outside of the tunnel. The air flow rate passing through the ventilating orifice was measured with Fischer-Porter flowmeter and the cavity air supply rate was then determined at the ambient conditions in the tunnel by applying the proper corrections for line pressure and temperature. Some ten different arrangements of ventilating orifices were finally used. These are tabulated in Table A-2.

The air pressure within the ventilating cavity was measured with an external water manometer. Before each cavity pressure measurement was made, the line connecting the manometer to the cavity was purged with gas to free it of any water droplets.

2.4 - Force Measurements

The forces acting on the ring wing were measured with the centrally mounted strain gage balance. This balance, made by the Task Corporation, is a six-component electrical strain gage balance. In the present work, however, only three force components were used: lift normal to the upstream flow, drag, and pitching moment. For use in this application the strain gage balance had to be waterproofed and protected against extraneous forces which could be introduced by the tubes transmitting the air supply to the ring wing. This turned out to be a simple problem for the present experiments; the air lines connecting the model support to the ring wing were made with flexible "Tygon" tubing and no appreciable interaction from this source was observed. The interior of the strain gage balance was maintained at a pressure approximately one ft. H_2O higher than the ambient pressure in the tunnel. This pressure was monitored on

an exterior water manometer and was maintained constant so that a spurious drag tare would not be encountered.

2.5 - Tunnel Corrections

As can be seen from Figure 1, the force balance and model are pitched to go about the tunnel center when the model is set with an angle of attack. The force balance in this arrangement measures forces in body axes rather than tunnel axes, and variable contributions of the weight of the model and balance are experienced for different angles of attack. These forces were measured with the complete assembly submerged in still water for the various angles of attack used and the results were then used to correct the observed forces to tunnel axes. No determination of any possible tare force due to the model support strut was made. No tunnel blockage corrections were made to the subsequently calculated data.

3. Results

3.1 - Fully Wetted Measurements

Lift coefficient, drag coefficient and moment coefficient in fully wetted flow at a Reynolds number of 6×10^5 are shown on the ring as a function of the angle of attack in Figure 2. Two sets of points are shown. The open ones are those which have the trip wire in place and the closed ones do not have the trip wire. It can be seen that the effect of the trip wire significantly increases the slope of the lift and moment curves. The drag coefficient is also affected somewhat. It will be noticed that zero lift does not occur precisely at zero angle of attack. The primary reason for this is that the adjacent free surface permits a distortion of the flow which is dependent upon Froude number. Nevertheless, the offset is relatively slight, being less than one-half degree, and the value of the lift slope agrees closely with the theoretical predictions of Weissinger (Ref. 7). In fact, the measured lift-slope is 1.43 and the theory of Weissinger including the effect of the central body gives 1.44.

The data shown in Figure 2 are corrected for the tare forces on the sting balance. These were obtained by removing the ring wing assembly and measuring the lift, moment and drag on the sting balance alone as a function of angle of attack.

3.2 - Steady Ventilation Measurements

As mentioned before, some ten different ventilating orifice patterns or configurations were used in this work. The first four of these (see Table A-2 of the Appendix) consist of a varying number of ventilating holes drilled into the original plenum provided in the ring wing. The planview of this plenum chamber can be seen in the upper diagram of Figure A-2. These four different configurations consist of 1/32 inch orifices being drilled into the rather small plenum chamber. In configuration No. 1 such holes spaced at one inch intervals are used. In the three subsequent arrangements using this plenum nine, five and three 1/32 inch orifices are used. In these cases the spacing between the orifices is 1/8 inch and for all cases the orifices are 1.2 inches from the leading edge.

The effect of ventilation with these four configurations in steady flow is summarized in Figures 3 through 7. In Figures 3, 4 and 5 are plotted the lift coefficient, drag coefficient and moment coefficient respectively for the various fixed angles of attack and for various ventilation parameters. In each case and for all the angles of attack, the introduction of the ventilating gas gives an increase in lift coefficient with a decrease in ventilation parameter K. Typical cavity lengths range from two to three chords and the length of cavity increases with decreasing ventilation parameter. No measurements of cavity lengths were made, however. The drag coefficient shows a slight increase with the presence of a cavity, although not an appreciable one, and the moment coefficient for each angle of attack decreases with ventilation. The lift results are smoothed and faired and are presented in summary in Figure 6. There it can be seen that the effect of ventilation, especially for configuration No. 1, causes an offset in the angle for zero lift on the complete ring wing of approximately three degrees, though this

amount decreases for smaller cavities (larger ventilation parameters) and also decreases with hole spacing having a smaller peripheral extent, i.e., hole patterns No. 2, 3 and 4. The slope of the lift versus angle of attack line is somewhat reduced for selective ventilation.

The ventilation parameter K is often used to characterize the flow in cavitation and ventilation experiments. However, in the present case it is perhaps of greater concern to a possible user to know the amount of ventilating gas required. The ventilating gas requirement is expressed in terms of the dimensionless flow coefficient, C_Q. This coefficient is a kinematic quantity being in essence the ratio of two velocities, that of the ventilating gas speed through the reference area to the freestream tunnel speed. There is undoubtedly some effect of gravity and other fluid properties in the present experiments on determining the magnitude of this flow coefficient, but separate experiments to determine these effects were not carried out (see for example Reference 8). Air flow rate coefficients for the first four ventilating hole configurations are presented in Figures 7a, 7b and 7c. It can be seen there that the amount of ventilating gas corresponds to a flow coefficient, C_Q, of approximately 1 or 2×10^{-3}. (Coefficients larger than about 2.5×10^{-3} were unable to be obtained with the original plenum chamber design.) Nevertheless, a flow coefficient of 1×10^{-3} is still sufficient to cause a substantial lift increment. As indicated above this value of C_Q can be interpreted as a flow of gas through the disk area of the ring at the ambient pressure of the ring at a speed of 10^{-3} times that of the freestream speed. From this it may be judged that a very small mass of ventilating gas would be required if the ambient pressure is not too much greater than atmospheric pressure.

It is of interest to observe the cavity formed by the various patterns of ventilating holes. Figure 8 shows three photographs of the selective ventilation on the ring wing at zero angle of attack for hole configurations No. 2, 3 and 4, with a ventilation parameter of

0.055. It can be seen that in each case a smooth gas cavity is formed and that the only significant difference between these three configurations is that the width of the cavity is increased with increasing number of holes. The angle of spread of the cavity in each case was approximately 25 degrees from the centerline. This is in agreement with some of the observations made in Reference 2, though the latter are on two-dimensional foils. It was also interesting to observe that the first hole configuration which has the ventilating orifices spread over a distance of two inches gives a substantially greater lift increment than any of the subsequent configurations. From Figure 3 we can see that at the lower ventilation parameter the configuration No. 2 gives a slight increase over that of configurations No. 3 and 4. It thus appears that the size of the ventilated cavity is thereby related to the amount of lift increment obtained through the ventilation.

3.3 - Magnitude of the Ventilation Effect on Lift

It would be a formidable problem to treat by means of lifting surface theory the effect of the presence of a ventilated cavity of the type seen in Figure 8 even on a two-dimensional hydrofoil of infinite aspect ratio, let alone to treat its effect on a ring wing which in itself is already reasonably complex. The ventilated cavity gives rise to strong local gradients of induced velocity and of trailing vorticity as can be seen in Figure 8 where sharply defined trailing vortices can be seen streaming downstream of the cavity. Though a complete theory may yet be developed, it would still be useful to have an estimate, however rough, of the magnitude of this effect for purposes of preliminary design. For the present one must of necessity rely upon empirical or semi-empirical approaches; even these are sparse and only Reference 2 deals with this problem. There, it is stated that the lift experienced by a partially ventilated hydrofoil of finite aspect ratio is equal to a fraction of the lift of a two-dimensional ventilated hydrofoil and to a fraction of the two-dimensional fully wetted hydrofoil lift. The fraction in each

case is the length of trailing edge of the hydrofoil covered by the ventilated region on the one hand and the fully wetted flow on the other divided by the total trailing edge length or span. Presumably one could extend this prescription to that of a ring wing if each of these lift coefficients were known in axisymmetric flow rather than two-dimensional flow. We are hindered in applying this formula in the present instance because we do not know what the lift coefficient would be for a Clark Y profile in two-dimensional ventilated flow. However, for the purpose of making an estimate we will assume that the present profile shape is under the action of ventilation similar to that of Hydrofoil A in Reference 2 operating at the same lift coefficient ($C_L = 0.5$). It is shown in Reference 2 that two-dimensional ventilation of its "Hydrofoil A" at a ventilation location equal to that of the present experiments reduces the lift coefficient to zero. The 10 percent Clark Y airfoil in axisymmetric flow should have a lift coefficient similar to that of a two-dimensional foil near the ground with a height-chord spacing the same as that of the present experiments. The lift coefficient for the present section under these conditions is 0.53. (We are indebted to Mr. J. Giesing of Douglas Aircraft Company for this calculation.) The extent of the ventilating region covering the trailing edge is then estimated from the observed spreading angle. We now make an estimate of the ventilation effect on the ring wing by assuming that the radial force coefficient of 0.53 is directly radially outward all around the wing except for that portion of the trailing edge covered by the ventilated cavity, where we assume the radial lift would be zero. The unbalanced force so calculated gives a lift coefficient of 0.027. Lift increments in the present work are observed to range from about 0.027 to 0.06, depending upon the amount of ventilating gas. The latter values, yet to be discussed, occur at much higher flow coefficients than have been discussed thus far. The lower values are typical of those observed in Figure 3 for hole configurations No. 2, 3 and 4. The higher lift increment observed

for configuration No. 1 would be in accord with the ideas discussed above because it covers a substantially larger amount of the periphery of the trailing edge. The order of magnitude then of the lift effect is in accord with the notions of Reference 2 and may suffice for a rough estimate at least for the time being.

We now turn to interference effects and the transient measurements that were carried out with the first four hole patterns.

3.4 - Interference Effects

If the ventilation technique is to be used for a control function it would be necessary to have controls in the horizontal direction as well as in the vertical direction as seen in Figure 8. This raises the possibility that two adjacent regions of ventilation would be used at the same time to effect a combined vertical and lateral force on the ring. The question then arises as to whether the two ventilating regions would interact with each other in any deleterious manner. This point was briefly investigated only to the extent of introducing an additional supply of ventilating air located 90 degrees from the original ventilation orifices by means of a rear mounted sting which was situated close to the ring. The experimental arrangement can be seen in Figure 9. In photograph (a) of Figure 9 no gas is being supplied through the auxiliary sting and in (b) the ventilating gas is turned on. The two cavities are seen to be similar. In the process of turning on the auxiliary supply of gas, the forces in the vertical plane, that is, the normal plane of making the lift measurements, are monitored. It was found that there was no observable change of force in the vertical plane (i.e., lift force) whether the auxiliary supply of gas was on or not. Similarly, we could not detect any change in the appearance of the lower cavity whether the auxiliary supply was on or not. From this we conclude that interference effects, if they exist, are quite small and that if the hydrofoil is properly designed and if the extent of ventilation is not too great, such mutual interference effects will not be a serious problem.

3.5 - Ventilation Decay

We now turn to a consideration of the transient effects that occur and in this section discuss some aspects of the termination process of the ventilation. With reference again to Figure A-1, it can be seen that a small shuttle valve is inserted just upstream of the plenum within the ring wing. The purpose of placing this small valve so close to the ring is to have the smallest possible reservoir of gas upstream of the ventilating orifices themselves. Then when the valve is closed and the air supply is cut off the cavity should be swept neatly away, thereby restoring the flow to its initial fully wetted condition as quickly as possible. This is precisely what happened, as can be seen in the photographs of Figure 10. (This sequence of photographs was arranged from a number taken at random.) Only one ventilating port is used in Figure 10 though similar results were obtained with the other hole configurations so far discussed. In any event it can be seen that when the supply of gas is terminated, the cavity breaks away cleanly from the surface of the ring wing. It should be mentioned that in Figure 10 the trip wire is being used.

The effect of this clean cavity breakaway on the force was examined by putting the output of the strain gage balance on an oscilloscope. Force traces corresponding roughly to the sequence shown in Figure 10 are shown in the upper trace of Figure 11(a) and 11(b). There time increases to the left and in the upper traces we see that the force suddenly decreases to a new level when the ventilation is stopped (the "hash" in the traces is pick-up). The time scale on these photographs is 0.2 seconds per major division and by close inspection of these traces as well as visual examination of the cavity, it is seen that the force decay is essentially complete within 50 milliseconds. This is the length of time required for the freestream velocity to travel a distance of three chords; it would be difficult to improve upon this result by mechanical means.

Similar decay experiments were also made at the same speed without the trip wire. It was found then that upon closure of the shuttle valve the ventilating gas would often not leave cleanly, but instead would flash around the entire ring in patches. On other occasions a portion of the gas cavity would be shed off and the remainder would stay attached to the ring and would slowly erode away. In these cases the force decay might take many seconds before being complete and in those situations where a patch of cavity ran around the ring a major force perturbation in directions other than the desired one would be experienced by the ring. It seemed clear that without the trip wire the cavity was being maintained in its position upon termination of the gas supply by means of an upstream separation. An example of this is shown in the photograph of Figure 12(a). Such incomplete shedding of the cavity causes slow and even erratic forces, as can be imagined. A further example of this is shown in the oscillograph trace in Figure 12(b). The conditions are the same as those of Figure 11 except that the trip wire is removed and the angle of attack of the ring is 4 degrees. A similar but not quite so undesirable a decay is shown in the force trace of Figure 12(c) where again the termination process is more lengthy than it should be.

In summary it appears to be very easy to ensure a clean shedding or separation of the cavity at the termination of ventilation when the liquid flow is always attached to the profile. For this reason extensive studies of cavity termination were not undertaken. We now pass on to the question of the start-up transient.

3.6 - Ventilation Initiation

In these first experiments covering the behavior of the first four configurations of Table A-2, ventilation initiation experiments were carried out on configurations No. 1 and 2 and examples of these are shown in the lower traces of Figure 11. There it may be seen that the length of time required to build up the force caused by the selective ventilation to its ultimate value is approximately one second. The initial rate of growth of this build-up process is quite

rapid and for the three cases shown approximately one-half of the ultimate lift force is developed within 0.1 second. It is interesting to note that in Figure 11(c), which is configuration No. 1 at a much lower tunnel speed, the rate of build-up is approximately the same as that of configuration No. 2 at the higher tunnel speed. The rather lengthy time required to establish these ventilating flows was somewhat unexpected. A possible cause for this long build-up time was thought to be due to the limitation in the maximum air flow rate that could be supplied to the ventilating ports with the original plenum chamber design. To obviate this limitation the support strut containing the shuttle valve and main air supply and the plenum chamber within the ring wing itself were then entirely redesigned to permit higher air flow rates. The diameter of all internal flow passages was increased at least by a factor of two and these new arrangements can be seen in the lower diagram of Figure A-2 in the Appendix. The increase in the internal diameter of the supply air system resulted in better than a tenfold increase in the supply of air available to the ventilating orifices, but it meant that the quick closing shuttle valve had to be abandoned. In its place and external to the model support system was installed a solenoid operated quick-opening valve. To have some idea how fast this valve could be opened, a quartz pressure pick-up was mounted in the main air supply line just downstream of the solenoid operated valve. It was found that under a wide range of inlet air pressure, the valve would open in a time somewhat less than 50 milliseconds. By this means it was possible to admit a sudden supply of air to the plenum chamber within the ring wing so that initiation studies could be continued but the ventilation termination experiments had to be discontinued. The plenum chamber was also considerably enlarged as can be seen from Figure A-2 so that different types of orifice patterns could be drilled on the surface of the ring wing. Following this modification the remaining six additional ventilating hole configurations of Table A-1 were experimentally studied. All of them were intended basically to

provide the possibility of a greater flow of air over a larger area of model.

The first configuration studied, No. 5, consisted of a single elongated hole (see Figure A-2) having an area equal to that of the internal supply lines. The subsequent modifications, Nos. 8 to 10, in essence spread out this orifice area over a larger portion of the ring. Before examining in detail the transient characteristics of these new hole configurations, we will pause to reconsider the forces generated in steady state ventilation as they are slightly different than those of the first four hole configurations. Lift coefficient and drag coefficient are plotted versus angle of attack for various air flow coefficients for each of these hole configurations and the results are summarized in Figures 13 through 18. In each of these the tunnel speed is 11 feet per second and the trip wire was used in all cases. It can be seen that there are distinct differences between the various hole configurations, the most noticeable one being that of configuration No. 6 which is shown in Figure A-3. In this the air stream issuing from the single hole is deflected downstream by means of a deflector. For this configuration we see in Figure 14 that there is a substantial reduction in performance compared to the other configurations. The deflector was installed because it was noticed that when ventilation was initiated with the single hole, configuration No. 5, with the highest injection pressure, an air 'jet' normal to the surface of the wing was formed rather than a cavity of the type seen in Figure 8. It was thought that deflecting this jet rearwards would help in establishing the ventilated cavity and result in quicker start-up times. The gas flow at start-up and at the maximum air flow rate is choked at the orifices; the resulting high velocity airstream when directed rearwards does not seem to result in a ventilated cavity; instead it appears to entrain the surrounding liquid flow and form an ill-defined jet. At lower air flow rates, however, the deflector acted much the same as the single hole, though it was not as effective. Hole configuration No. 7 differs from that

of No. 6 only in that a part of the side of the deflector had been cut away to permit the air to stream more easily into the surrounding liquid flow as can be seen again in Figure A-3. The remaining hole configurations, Nos. 8, 9 and 10, are intended to distribute the supply of air over a larger portion of the ring surface and are further intended to have several orifices feeding into the same ventilated cavity rather than each orifice initiating a separate cavity as occurred in configuration No. 1. The drilling patterns for these configurations are shown in Figure A-4.

It is very clear from the results of these additional measurements that the magnitude of the air flow coefficient has an important though by no means dominant part in determining the increment in lift coefficient brought about by the ventilation. The influence of air flow coefficient is summarized for the various hole configurations in Figure 19 for zero angle of attack. The outstanding feature of this graph is that the ventilating air supply can be changed by two orders of magnitude and only change the lift coefficient by a factor of two. Except for two or three data points this trend is quite clear. It is significant from this figure that the most efficient use of ventilating gas is still obtained with hole configuration No. 1. It will be recalled that in this configuration the ventilating holes are spread out over a greater extent of the ring wing than any of the other configurations and tends to support the reasoning mentioned in Section 3.3. The lowest air flow rates that maintained a stable cavity were found for the single hole configurations No. 5 and 7. Perhaps the most efficient use of the air supply would be to use several such holes if larger forces are desired.

Photographs of the ventilation cavities on hole configurations No. 5, 7 and 10 for both large and small air flow coefficients are shown in Figure 20 for zero angle of attack. The appearance of the cavities of the remaining configurations is very similar to those shown except possibly for No. 6, the deflector. In this case the cavity is much narrower and is poorly defined for all but the lowest

air flow coefficient where it resembles that of No. 7. There is essentially little difference in the appearance of these cavities at the lower flow coefficients, but at or near the maximum air flow coefficients the single hole, configuration No. 5, appears to cause a large ragged cavity which does not attach itself well to the surrounding hydrofoil, but in any case the cavity is not well defined for any of the ventilation configurations at the highest air flow coefficients.

We now return to discuss the transient behavior of these additional air injection schemes. It was found straight off that air injection at the higher or highest flow coefficients available did not result in an appreciably more rapid build-up of the force than the original results of Figure 11. Instead, if anything it took longer to establish the ultimate force than before. Subsequent experiments were then carried out on all the hole configurations at low and intermediate rates of injection and some typical force traces for these are shown in Figure 21. In these oscilloscope photographs are shown two traces or in some instances two sets of traces. The upper one is in each case the time history of the lift force, the time increasing as before to the left, whereas the lower trace shows the pressure-time history of the air supply measured just downstream of the quick opening valve.* In all the cases shown in Figure 21 the initial air pressure rises quickly to the maximum air pressure available, around 80 psig. This pressure subsequently decays to a lower value depending upon the steady state amount of air supplied to the cavity. The largest air flow rates maintained this maximum air pressure at its full value. The lower flow coefficients were got by throttling the inlet supply line. There was a certain volume of air in the lines passing from the throttle valve to the quick opening valve and it is this volume which gives rise to the pressure decay seen in the traces of Figure 21. In any case whether the pressure was maintained at its maximum value at the highest flow coefficient

---

* The zero in each case is the short horizontal line at the right.

or was injected with an initial high rate which tapered off to its ultimate value, the shape of the force-time trace is always basically similar. Nevertheless, it can be seen that there is a definite trend; when the air is so injected the time required is significantly less for the lower air flow coefficients than for the higher ones. It is still rather difficult to establish an exact measure of this time because the steady state value is approached only asymptotically. For the purpose of making comparisons between these different hole configurations and their injection techniques, the time required to establish 50 percent and 70 percent of the ultimate force was measured on the oscilloscope traces and is tabulated in Table 1. There for various angles of attack and tunnel speeds these times are measured and reported in seconds. This time is also reported in chords traversed by the freestream speed although it is not known whether or not this is the right non-dimensional parameter to use. It should be mentioned that these measurements are not capable of great precision but they should serve as a good indication of the order of magnitude of the time required.

From Table 1, it is quite clear that the lower air flow coefficients require substantially less time than the higher air flow coefficients, especially for the 70 percent level. Depending upon tunnel speed and the particular configuration used, times as low as 50 milliseconds are observed for the lowest air flow coefficients and as long as 1-1/2 seconds required to establish 70 percent of the ultimate force for the highest air flow coefficients. The same trend is also observed for the time required to establish 50 percent of the ultimate force although characteristically this time is one-third or less than the time for the 70 percent level. There does appear to be systematic differences between the various configurations, those having the shortest time required for build-up being Nos. 7, 8 and 9. This time also depends somewhat on angle of attack, but more importantly on tunnel speed. Typically for the

70 percent level the time required at 22 feet per second is about twice or so longer than that required at equivalent conditions at 11 feet per second - though this observation does not appear to follow through entirely for at the 50 percent level a smaller dependence on tunnel speed is observed. Nevertheless it is generally true that a faster speed requires a longer time to build up the force.

As mentioned above these times are also interpreted in terms of chord lengths travelled by the flow. In some cases the shortest observed times correspond to a distance of only 1-1/2 chords but at the lower air flow coefficients it appears that the flow can be established within a distance of six chords. These values certainly imply that the speed of response of this type of control function would compare favorably with a mechanical control device. While the larger air flow rates tend to take excessive times regardless of the particular means of air injection, it may be possible to use these high values if desired because the time required to establish only 50 percent of the ultimate force is still comparatively short.

3.7 - Scaling Processes

As mentioned in Section 3.2, the steady state ventilation process is characterized by the ventilation parameter K which determines the pressure within the ventilated cavity. The air flow coefficient C_Q in the present experiments is mainly a function of the ring geometry, angle of attack, and of the ventilation parameter K. The mechanism of air entrainment for lifting surfaces in steady flow is fairly complex but the work of Reference 8 shows that at Reynolds numbers typical of the present work, C_Q depends mainly upon the ventilation parameter K and the Froude number. But in any case if the Reynolds number effect is not strong C_Q is essentially a volumetric process and thus for example does not depend upon the absolute magnitude of the ambient pressure. We can therefore characterize the steady state ventilation results of

the present experiments by the air flow coefficient C_Q or by the ventilation parameter K as they are related to each other. It should be clear that if the gas is a condensible one or if the density of the gas is comparable to the surrounding liquid flow, additional scaling parameters have to be included.

Under some conditions instabilities of ventilated flows are observed (Ref. 9) but none were observed in these experiments.

Scaling laws for the dynamic process of the start-up of the ventilated flow remain to be investigated. The transient data given in Table 1 for the various configurations are really not sufficiently fine-graded nor are there changes in model scale which would permit such scaling laws to be established. As already briefly discussed the time required to establish a certain fraction of the ultimate force does depend upon tunnel speed as well as the air flow coefficient. For example, for hole configuration No. 5 at speeds of 11 and 22 feet per second respectively and at the relatively high air flow coefficient $C_Q = 1.2 \times 10^{-2}$ the time to establish 70 percent of the ultimate force is 0.5 and 1.0 seconds respectively. However, the time to establish only half the ultimate force is the same at the two speeds, namely 0.2 seconds. It is difficult to imagine a kinematic process in which time would scale directly with the velocity. While it is generally true that higher tunnel speeds require longer times, the initiation of the process seems to be somewhat time-independent as some of the data for the 50 percent force level of configuration No. 10 show. But this point cannot be settled until dynamic scale experiments are undertaken for this specific purpose. Lacking this information, it can only be assumed on the basis of geometric similarity that the time required to establish the force should be proportional to the square of the length dimension divided by tunnel speed.

In an effort to understand somewhat more fully the physical events taking place during the start-up of the ventilation process, a few high-speed movies were taken and assembled into a short film

strip (Ref. 10). These motion picture photographs were taken of the ventilation process on hole configuration No. 10. It can be seen from these photographs that when the maximum air flow is injected into the originally fully wetted flow, the cavity grows quickly and to a greater extent than its ultimate size. But the surface of the cavity is not smooth and is extremely rough and corrugated. Initiation of cavities which have a lower C_Q on the order of 10^{-3} rather than 10^{-2} produce more smoothly growing cavities and apparently result in a less disturbed liquid flow about the profile. From this standpoint, hole configurations No. 8, 9 and 10 are probably superior to a single hole as the supply of air is spread over a larger area in the growth phase. Visual observations of the injection through hole configuration No. 5 under the maximum air flow rate revealed that a jet of air was shot into the surrounding liquid flow and it took a considerable length of time for this initial disturbance to pass away. Indeed this was the reason for the deflector study as previously mentioned. At such high initial rates of injection, the two-phase flow about the profile does not resemble the ultimate ventilated cavity that is produced and instead acts as if it were merely a jet issuing normally from the surface. However, data of Table 1 show that even for the single hole injection, if the steady state air coefficient is sufficiently low the ventilated pattern is established reasonably rapidly. This problem of initiation of the ventilating process clearly needs further attention, especially if one is interested in short reaction times.

All of the build-up times discussed so far have taken place with the air pressure within the lines supplying the ventilating cavity at its highest value - around 80 psig. This supply pressure then decayed to its steady state value for the lower air flow coefficients as seen in Figure 21. Additional experiments were made in which lower initial injection pressure (but having the same steady state air flow rate coefficient) were used. All of these resulted in longer build-up times.

4. Concluding Remarks

From the experimental data presented herein, sizable forces can be obtained by selective ventilation over a small portion of the circumference of a ring wing. These forces are thought to be sufficient to provide a useful control function, perhaps for an underwater body such as a torpedo. It would be desirable to carry out a refined calculation of the effect of selective ventilation on ring wings and other forms of hydrofoils with finite aspect ratio for the purpose of making more accurate design estimates.

This selective ventilation procedure seems to work well provided that the original fully wetted flow about the hydrofoil has no separation zones. Then the steady ventilation and the start-up and termination processes are all accomplished in an orderly manner. The termination process is quick and would be comparable to a movable surface type of control, but the start-up process does take a longer time and is apparently governed by dynamic processes not yet understood. Further work concerning the dynamics of the injection process for selective ventilation is certainly in order.

In either case, however, the selective ventilating process can be started and stopped within a time corresponding to the distance that the freestream velocity requires in travelling approximately 6 to 10 chord lengths which is a time sufficiently short to conceive of using this technique in a practical application.

Acknowledgment

The authors wish to acknowledge the assistance of T. Kiceniuk and E. R. Bate, Jr., in the design of apparatus for this experimental program; of H. Hamaguchi, J. Kingan and G. Lundgren of the Hydrodynamics Laboratory staff; and of C. Eastvedt for the photographic work. This program was supported by the Office of Naval Research under Contract Nonr 220(54) and administered under the technical direction of the Naval Ordnance Systems Command, Weapon Dynamics Division, Code ORD-035.

REFERENCES

1. Acosta, A. J., Kiceniuk, T., and Bate, E. R. Jr., "Measurements of Fully Wetted and Ventilated Ring Wing Hydrofoils", California Institute of Technology Hydrodynamics Laboratory Report No. E-138.1, 1965; also A.S.M.E. Paper 66-WA/UnT-4.

2. Lang, T. G., Daybell, D. A. and Smith, K. E., "Water-Tunnel Tests of Hydrofoils with Forced Ventilation", NAVORD Report 7008, November 1959; see also, Lang, T. G. and Daybell, D. A., "Water-Tunnel Tests of Three Vented Hydrofoils in Two-Dimensional Flow", J. of Ship Research 5, No. 3, December 1961.

3. U. S. Patent 3,096,739, Method and Apparatus for Steering Underwater Bodies, July 9, 1963, to Kenneth E. Smith.

4. "Supramar's PT 150-DC", Hovercraft and Hydrofoil 6, No. 9 June 1967, p. 25.

5. McRoberts, G. M., personal communication.

6. Fabula, A. G., "Linearized Theory of Vented Hydrofoils", NAVWEPS Report 7637, March 1961.

7. Weissinger, J., "Some Results From the Theory of the Ring Wing in Incompressible Flow", Adv. in Aero. Sci., 2, Pergamon, 1959, pp. 798-831.

8. Campbell, I. J. and Hilborne, D. V., "Air Entrainment Behind Artificially Inflated Cavities", Second Symposium on Naval Hydrodynamics, Office of Naval Research ACR-38, 1958.

9. Silberman, E. and Song, C. S., "Instability of Ventilated Cavities," St. Anthony Falls Hydraulic Laboratory Technical Paper No. 29, Series B., University of Minnesota, 1959.

10. Acosta, A. J. and Wade, R. B., "Partial Ventilation in a Ring Wing", Film Report No. 74 , Hydrodynamics Laboratory, California Institute of Technology, August 1967.

TABLE 1

BUILD-UP TIME AND LIFT INCREMENTS FOR VARIOUS VENT HOLE CONFIGURATIONS

Vent Hole Designation	Tunnel Speed ft/sec	Angle of Attack deg.	ΔC_L	C_Q	$\tau_{.7}$ sec.	$\tau_{.7}$ chords	$\tau_{.5}$ sec.	$\tau_{.5}$ chords
1	10	0			0.2	6		
2	18.5	0	0.040	2×10^{-3}	0.15	8.3		
5	11	0	0.032	2×10^{-4}	0.1	3.3		
5	11	0	0.045	1.2×10^{-2}	0.5	16.6	0.2	6.6
5	11	0	0.056	2.5×10^{-2}	1.0	36	0.2	6.6
5	11	0	0.065	4.6×10^{-2}	1.5	50	0.5	16.6
5	22	0	0.027	6×10^{-4}	0.2	13		
5	22	0	0.045	0.6×10^{-2}	0.8	53	0.15	10
5	22	0	0.052	1.3×10^{-2}	1.0	66	0.2	13
5	22	0	0.062	2.0×10^{-2}	1.3	86	0.3	20
5	11	-3	0.027	2.8×10^{-4}	0.1	3.3		
5	11	-3	0.048	1.2×10^{-2}	0.5	16.6	0.15	5
5	11	-3	0.060	2.5×10^{-2}	0.5	16.6	0.15	5
5	11	-3	0.068	4.6×10^{-2}	0.8	26	0.2	6.6
5	11	-3	0.029	6×10^{-4}	0.2	13	<0.1	6.6
5	11	+3	0.027	1.9×10^{-4}	0.2	6.6		
5	11	+3	0.039	1.2×10^{-2}	0.3	10	0.1	3.3
5	11	+3	0.049	2.5×10^{-2}	1.0	33	0.4	13.2
5	11	+3	0.063	4.6×10^{-2}	1.5	50	0.4	13.2
7	11	0	0.032	1.9×10^{-4}	0.05	1.6		
7	11	0	0.044	1.3×10^{-2}	0.5	16	0.1	3.3
7	11	0	0.062	4.6×10^{-2}	1.5	50	0.2	6.6
7	22	0	0.034	7×10^{-4}	0.1	6.6		
7	11	-3	0.035	3.3×10^{-4}	0.05	1.6		
7	11	-3	0.047	1.3×10^{-2}	0.5	16.6	0.1	3.3
7	11	-3	0.053	4.8×10^{-2}	0.7	23	0.2	6.6
7	22	-3	0.032	7.5×10^{-4}	0.15	10		

TABLE 1 (continued)

BUILD-UP TIME AND LIFT INCREMENTS FOR VARIOUS VENT HOLE CONFIGURATIONS

Vent Hole Designation	Tunnel Speed ft/sec	Angle of Attack deg.	ΔC_L	C_Q	$\tau_{.7}$ sec.	$\tau_{.7}$ chords	$\tau_{.5}$ sec.	$\tau_{.5}$ chords
7	11	+3	0.030	1.9×10^{-4}	0.05	1.6		
7	11	+3	0.041	1.3×10^{-2}	0.20	6.6	0.1	3.3
7	11	+3	0.058	4.7×10^{-2}	1.2	36	0.2	6.6
7	22	+3	0.031	4.2×10^{-4}	0.15	10		
8	11	0	0.026	3.43×10^{-4}	0.05	1.6		
8	22	0	0.032	9.2×10^{-4}	0.06	4		
8	11	-3	0.025	2.3×10^{-4}	0.1	3.3		
8	22	-3	0.030	9.0×10^{-4}	0.15	10		
8	11	+3	0.023	3.0×10^{-4}	0.05	1.6		
8	22	+3	0.026	13.6×10^{-4}	0.04	2.6		
9	11	0	0.033	10.2×10^{-4}	0.06	2.0		
9	22	0	0.036	9.6×10^{-4}	0.1	7		
9	11	-3	0.034	9.7×10^{-4}	0.06	2.0		
9	22	-3	0.041	9.8×10^{-4}	0.2	13		
9	11	+3	0.025	10.1×10^{-4}	0.05	1.6		
9	22	+3	0.031	8.6×10^{-4}	0.1	7		
10	11	0	0.038	8.3×10^{-4}	0.1	3.3	0.05	1.6
10	22	0	0.037	6.0×10^{-4}	0.3	20	0.1	6.4
10	11	-3	0.045	8.3×10^{-4}	0.2	6.6	0.1	3.3
10	22	-3	0.043	5.8×10^{-4}	0.5	33	0.1	6.6
10	11	+3	0.031	7.5×10^{-4}	0.05	1.6		
10	22	+3	0.031	6.0×10^{-4}	0.05	3.2		

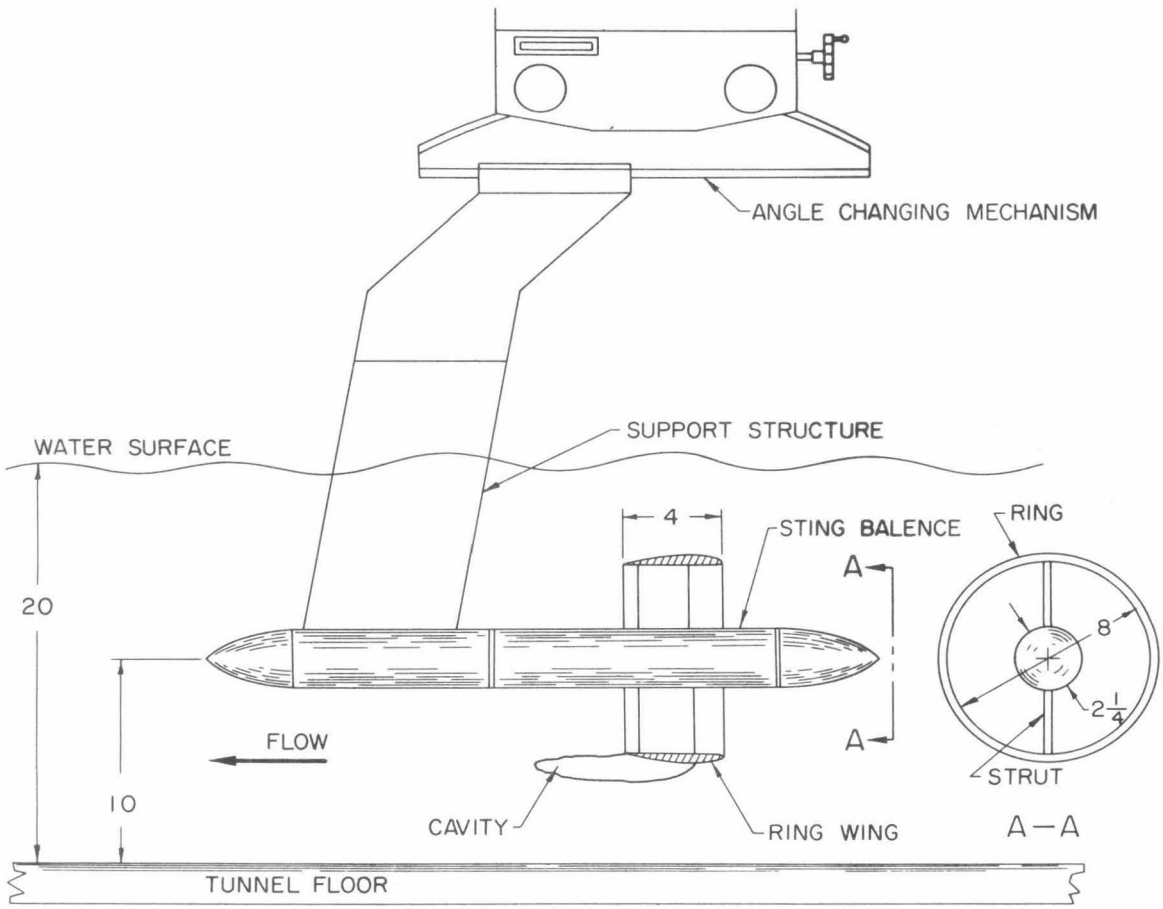

Fig. 1 - Sketch of ring wing assembly in tunnel

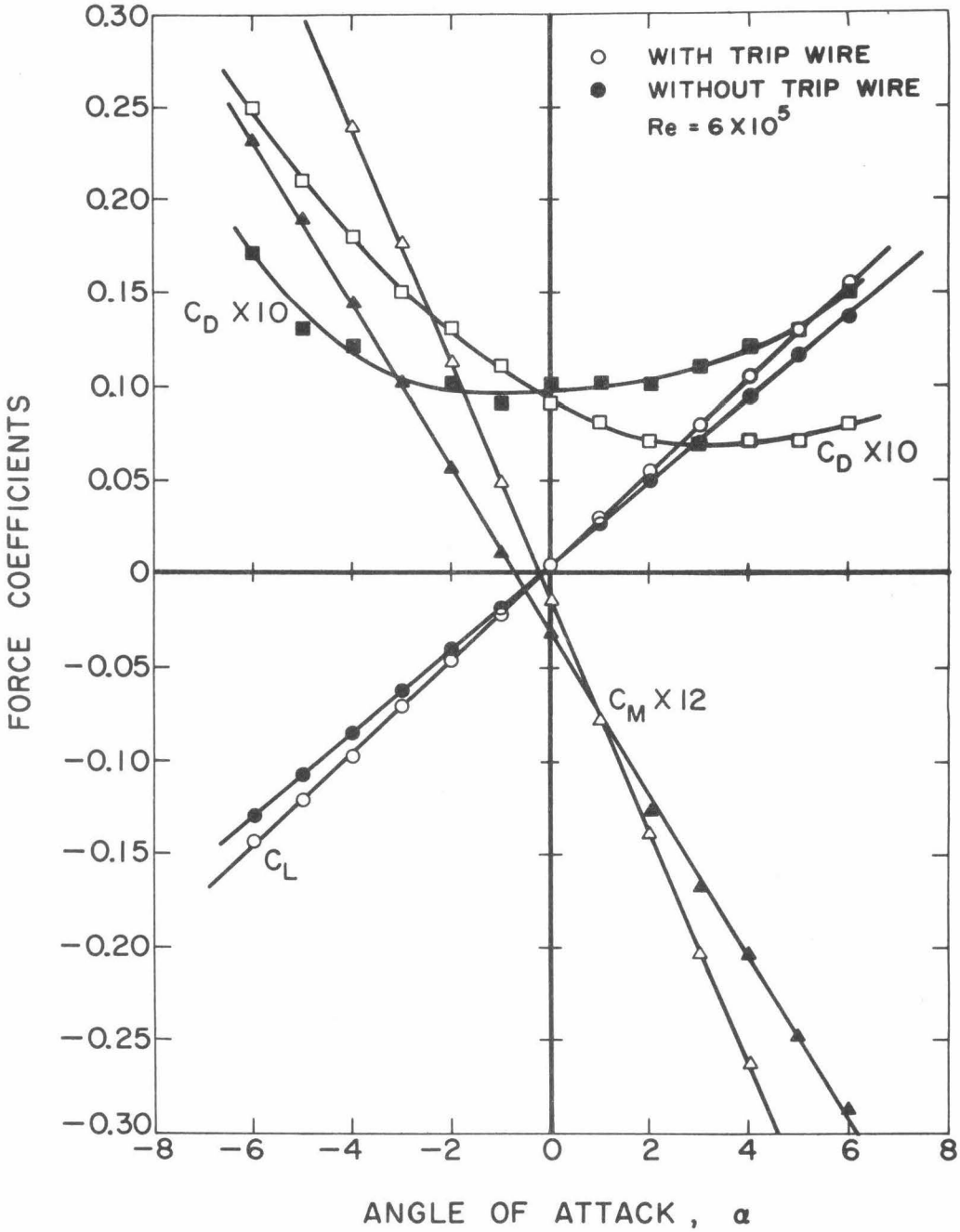

Fig. 2 - Force coefficient and moment coefficient of a ring wing in fully wetted flow as a function of angle of attack. Re = 6 x 10^5, the diameter of the ring is 8 inches, and the chord is 4 inches. The profile section is a 10 percent Clark Y.

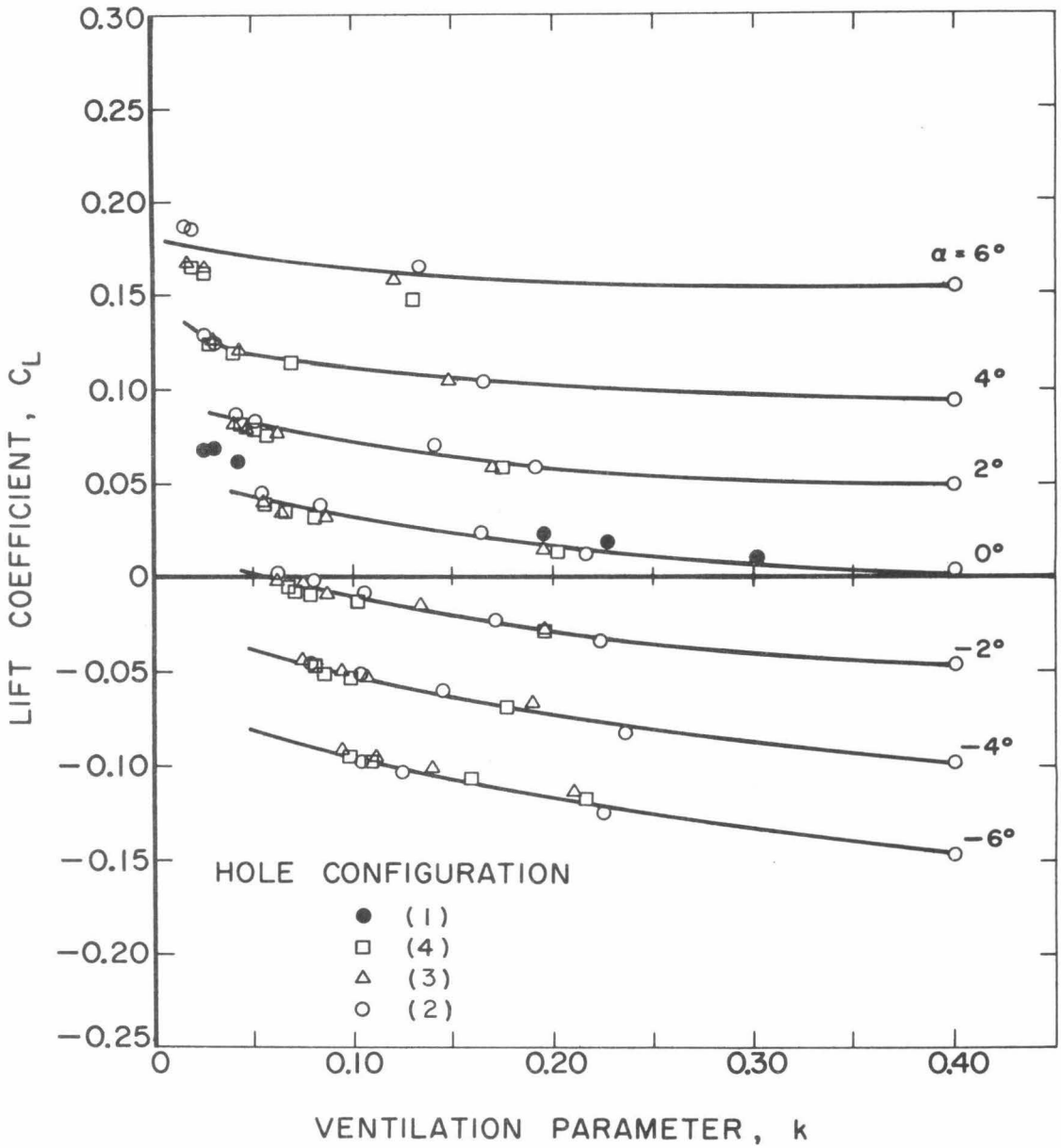

Fig. 3 - Lift coefficient versus ventilation parameter for various vent hole configurations. Re = 6×10^5.

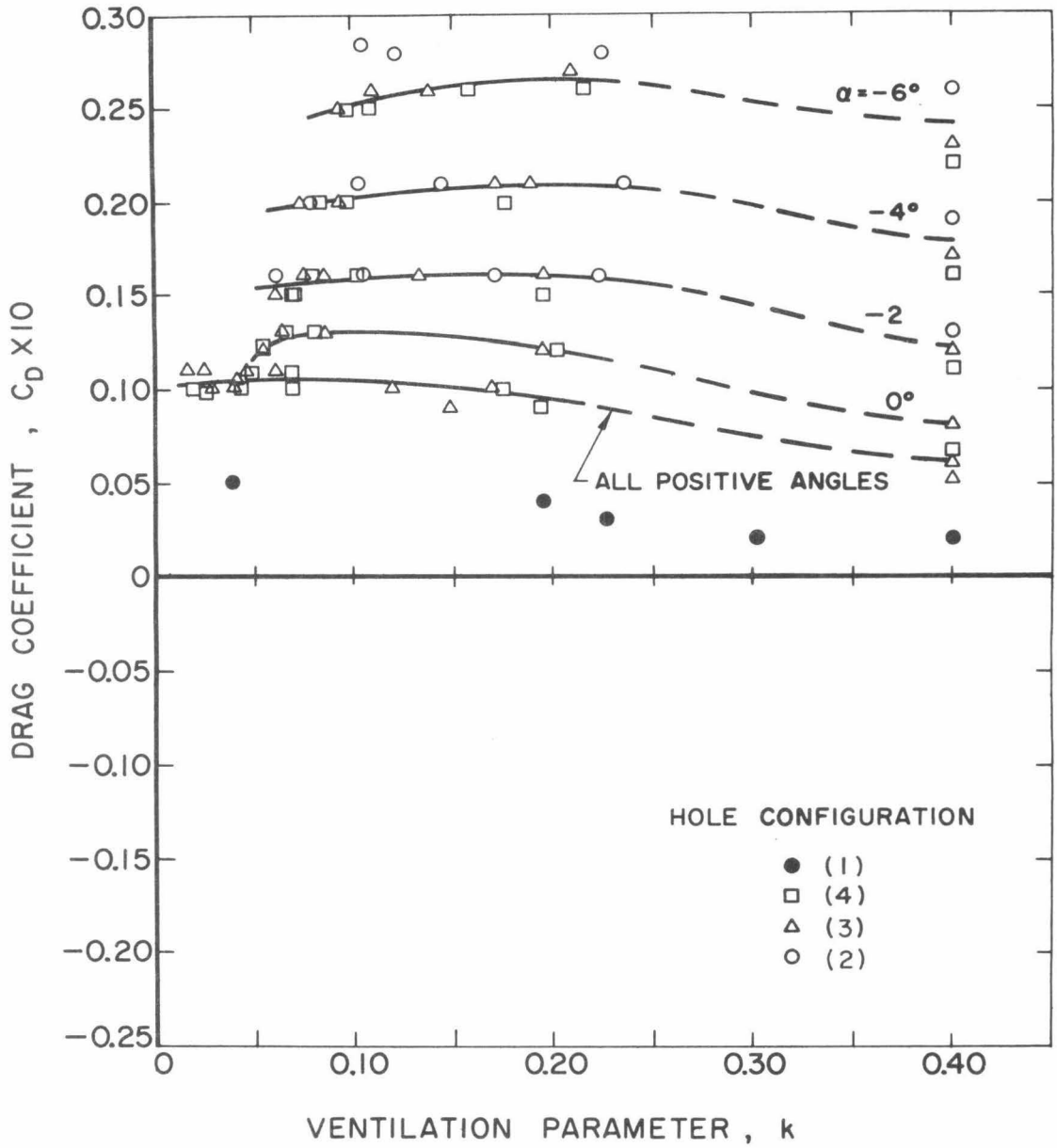

Fig. 4 - Drag coefficient versus ventilation parameter for various vent hole configurations. Re = 6×10^5.

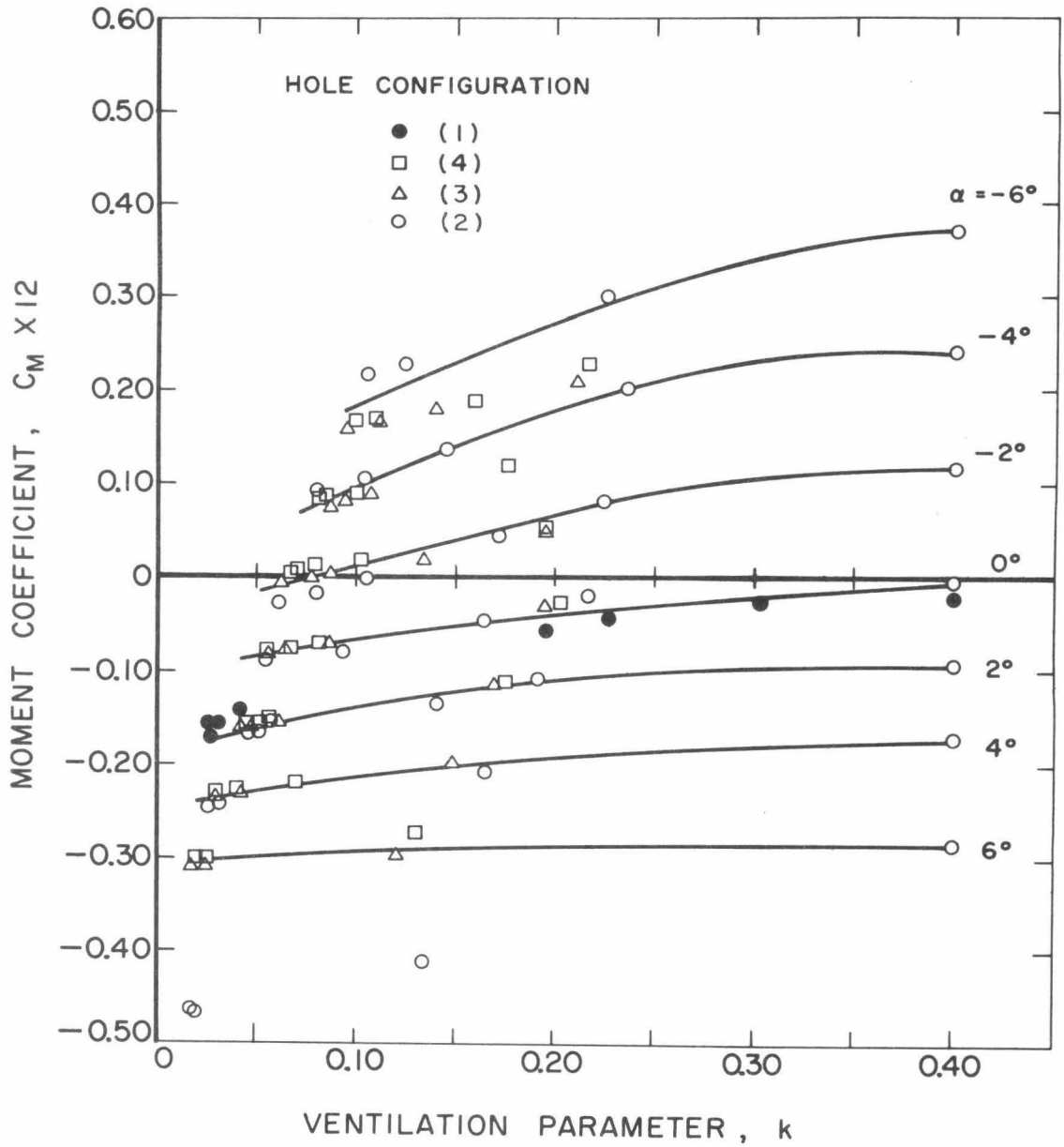

Fig. 5 - Moment coefficient about the leading edge versus ventilation parameter for various vent hole configurations. Re = 6×10^5.

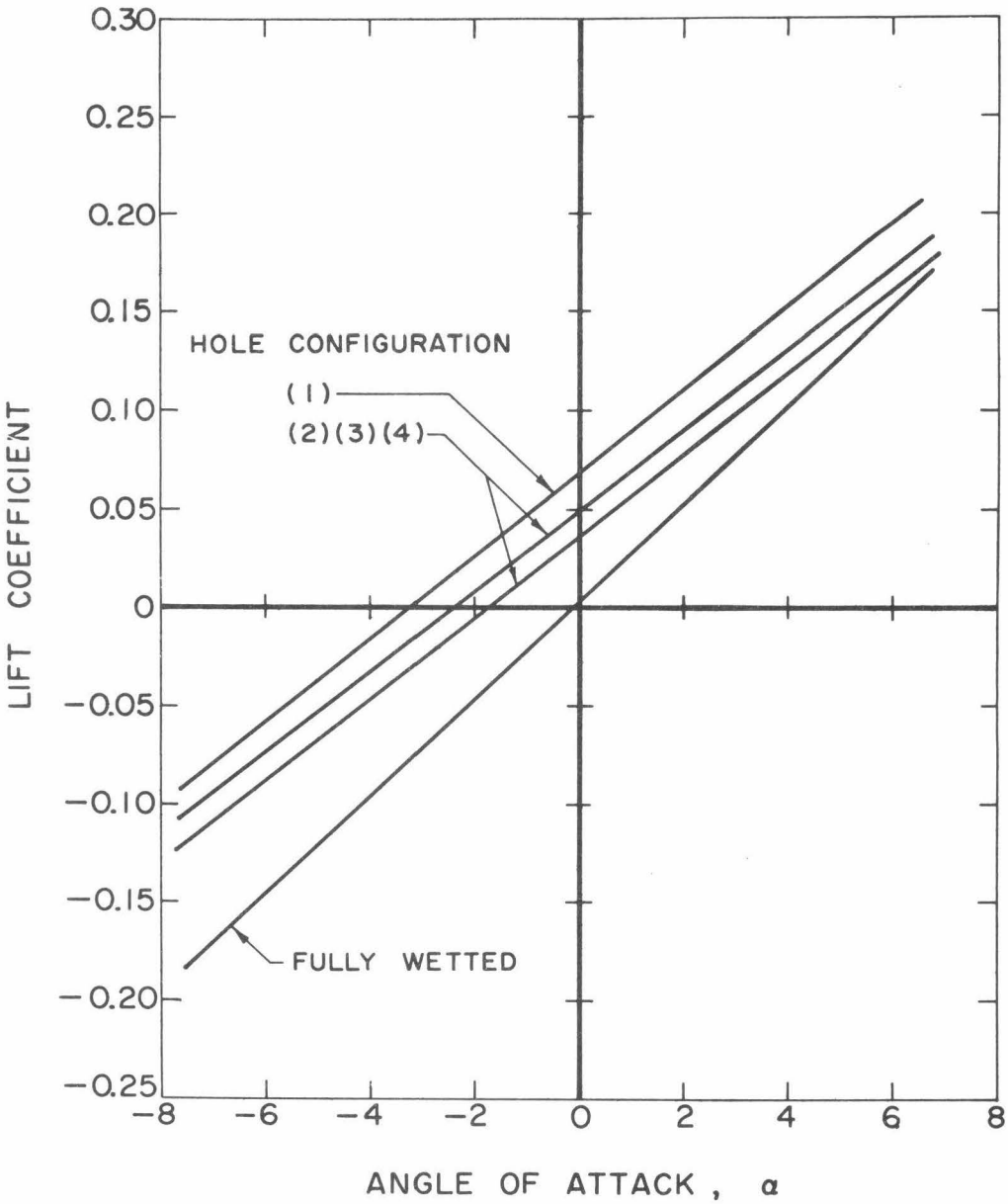

Fig. 6 - Effect of selective ventilation on the lift coefficient for the ring wing with various vent hole configurations. Re = 6×10^5.

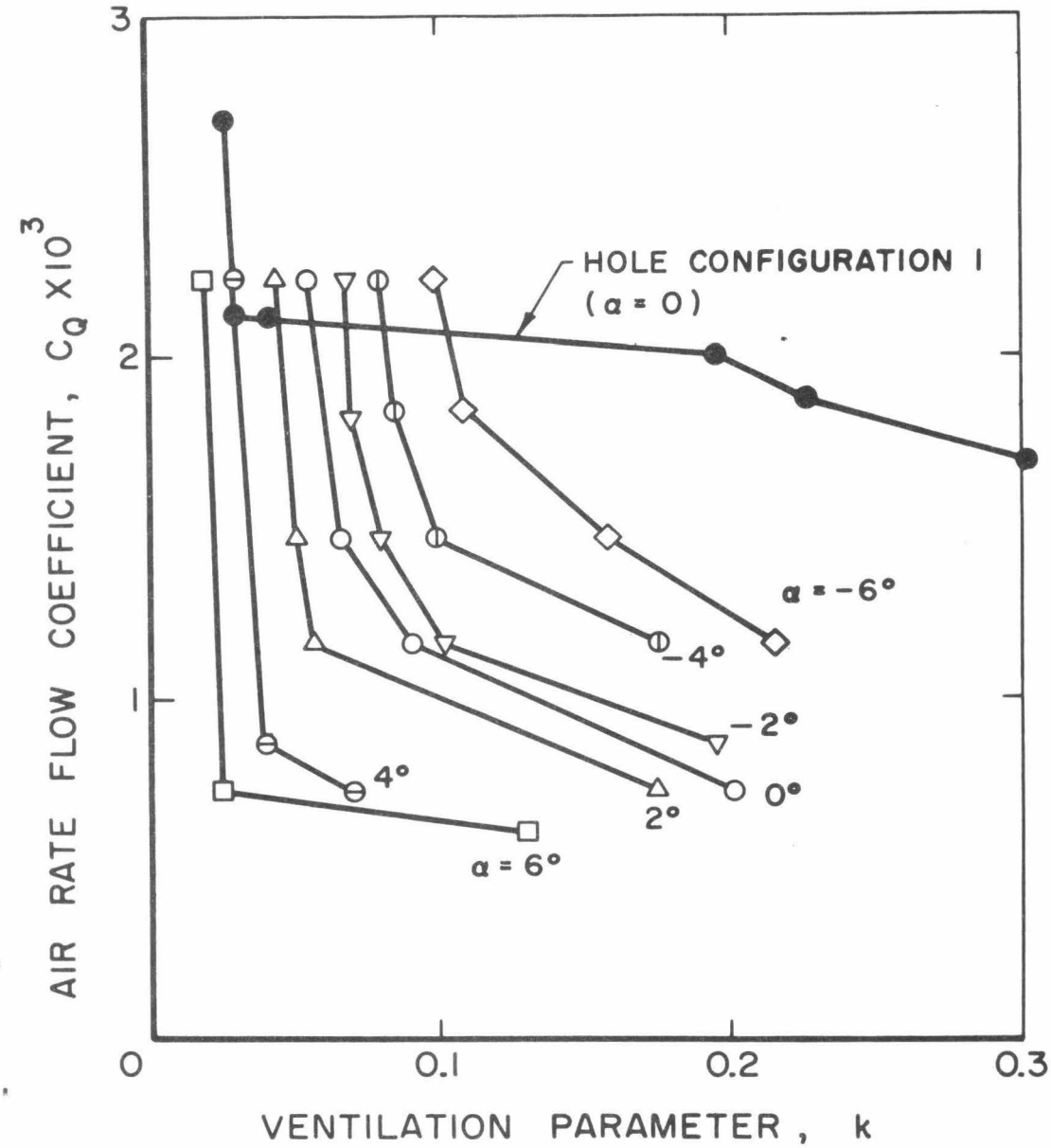

Fig. 7 - (a) Air flow rate coefficient versus ventilation parameter for vent hole configuration No. 4, three 1/32 inch holes at 1/8 inch spacing.

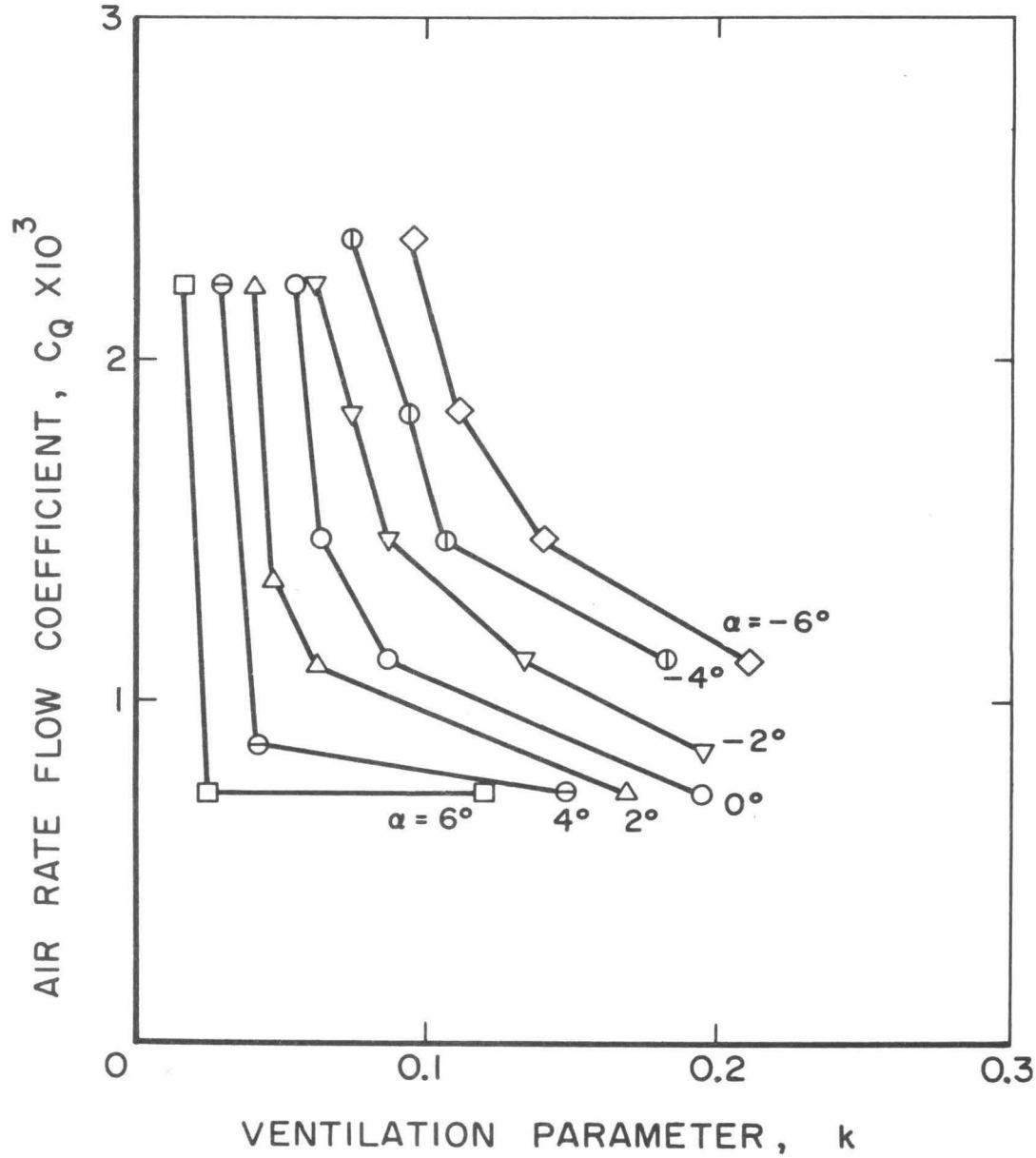

Fig. 7 - (b) Air flow rate coefficient versus ventilation parameter for vent hole configuration No. 3, five 1/32 inch holes at 1/8 inch spacing.

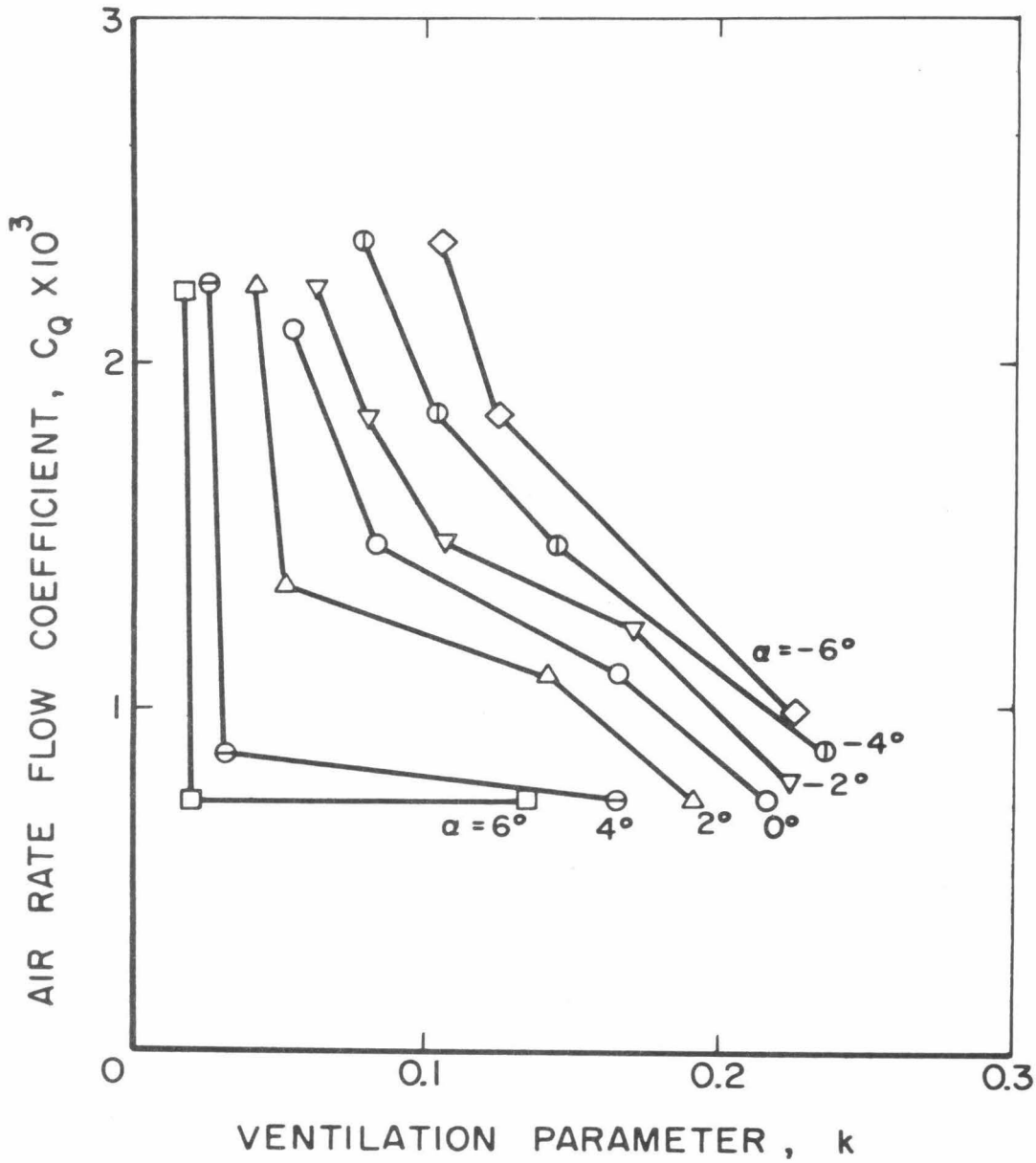

Fig. 7 - (c) Air flow rate coefficient versus ventilation parameter for vent hole configuration No. 2, nine 1/32 inch holes at 1/8 inch spacing.

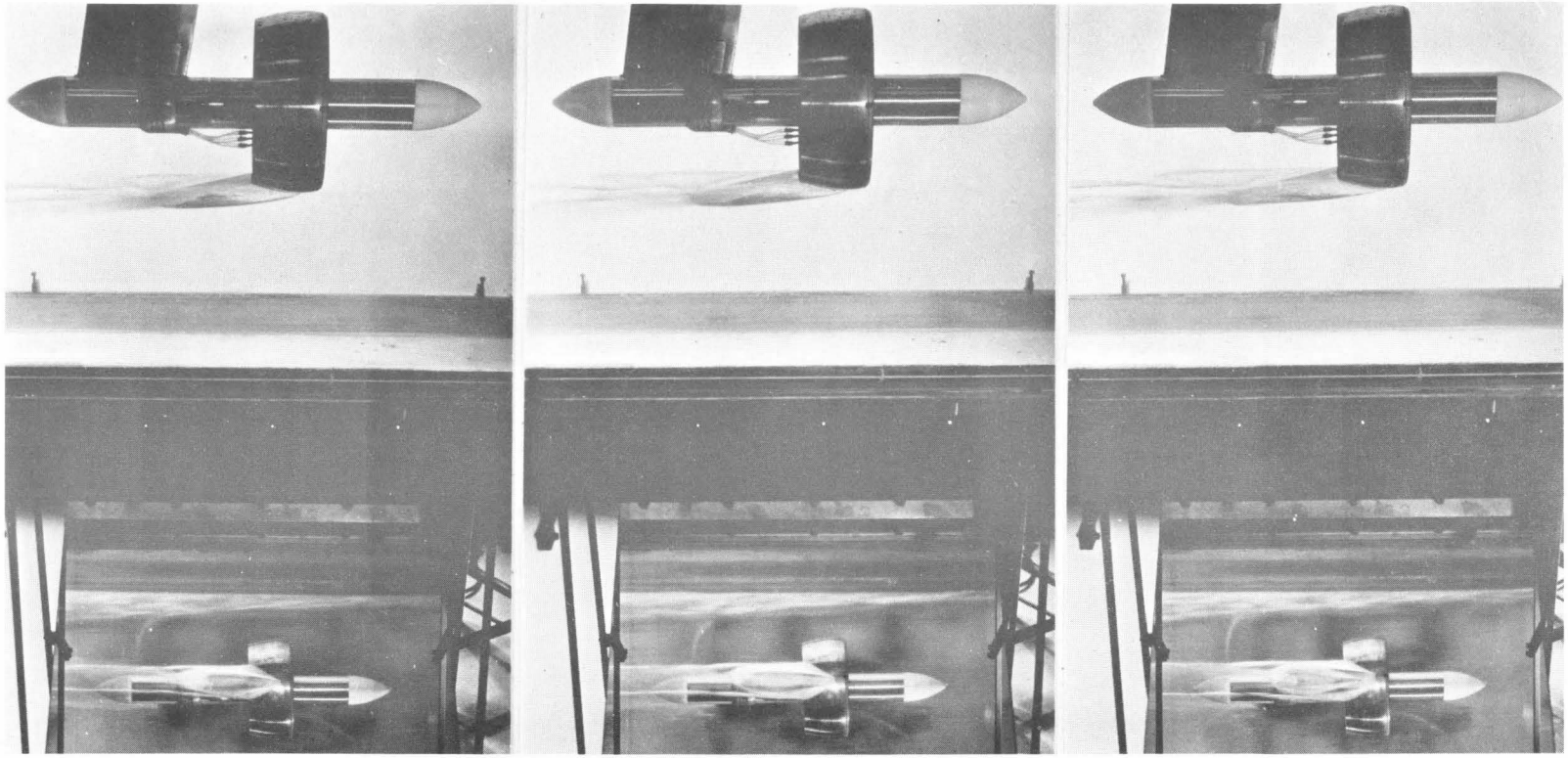

3 Holes 5 Holes 9 Holes

Fig. 8 - Photographs of selective ventilation on the ring wing at a speed of 18.5 feet per second and zero angle of attack for the Nos. 4, 3, and 2 hole configurations with a ventilation parameter of 0.055.

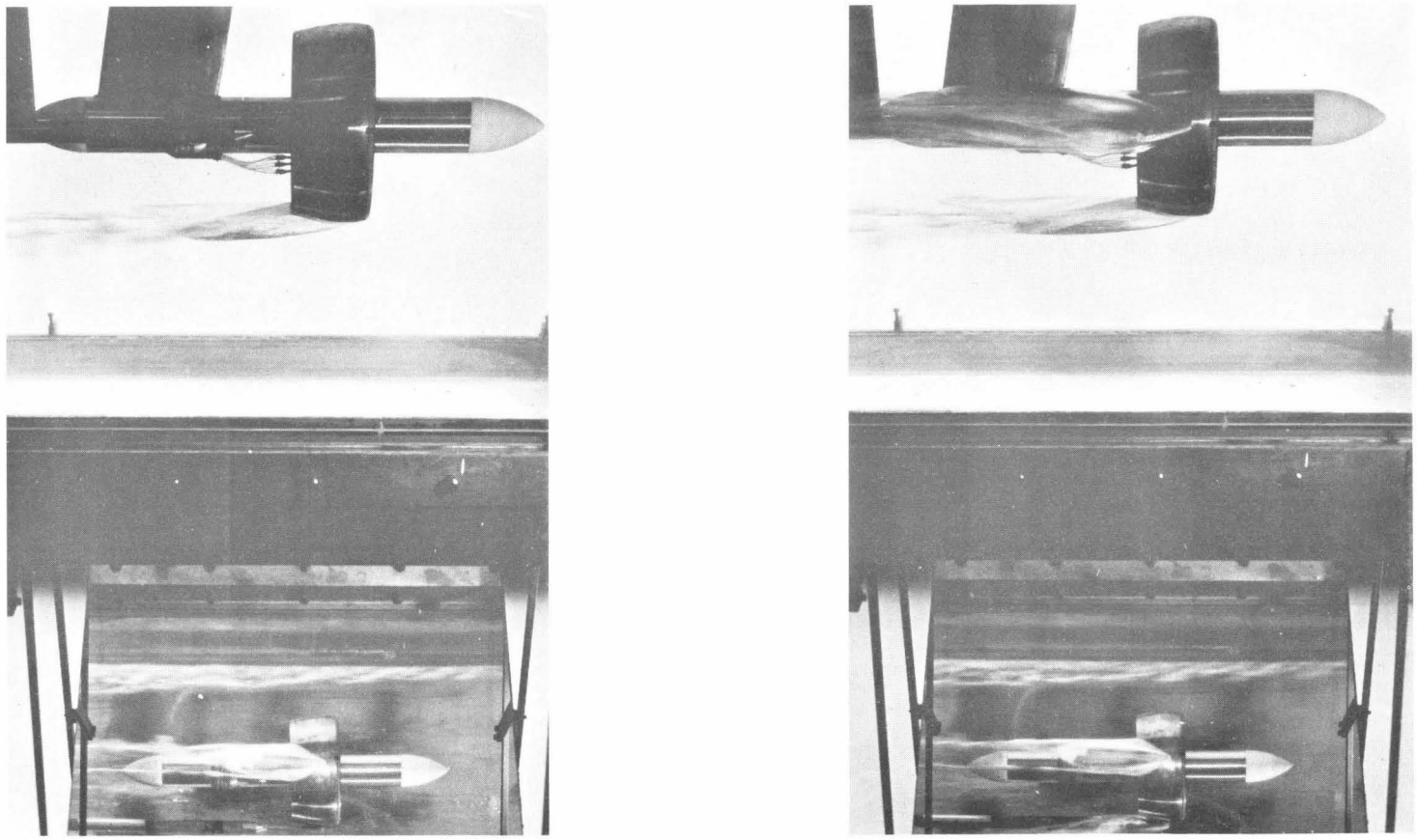

(a) (b)

Fig. 9 - Photographs showing that there is no interference between two ventilated cavities. In (b) the bottom cavity is unaffected by the presence of the side cavity.

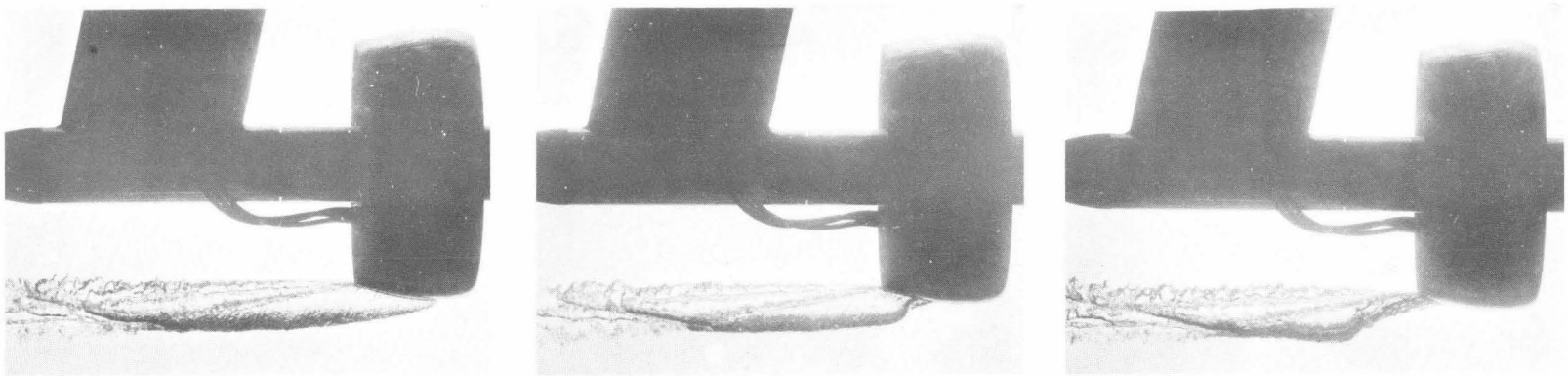

Fig. 10 - Photographs (taken at random) showing the sequence of cavity breakaway when the air supply is shut off. One ventilation hole is used, the angle of attack is zero degrees and the tunnel speed is 18.5 feet per second.

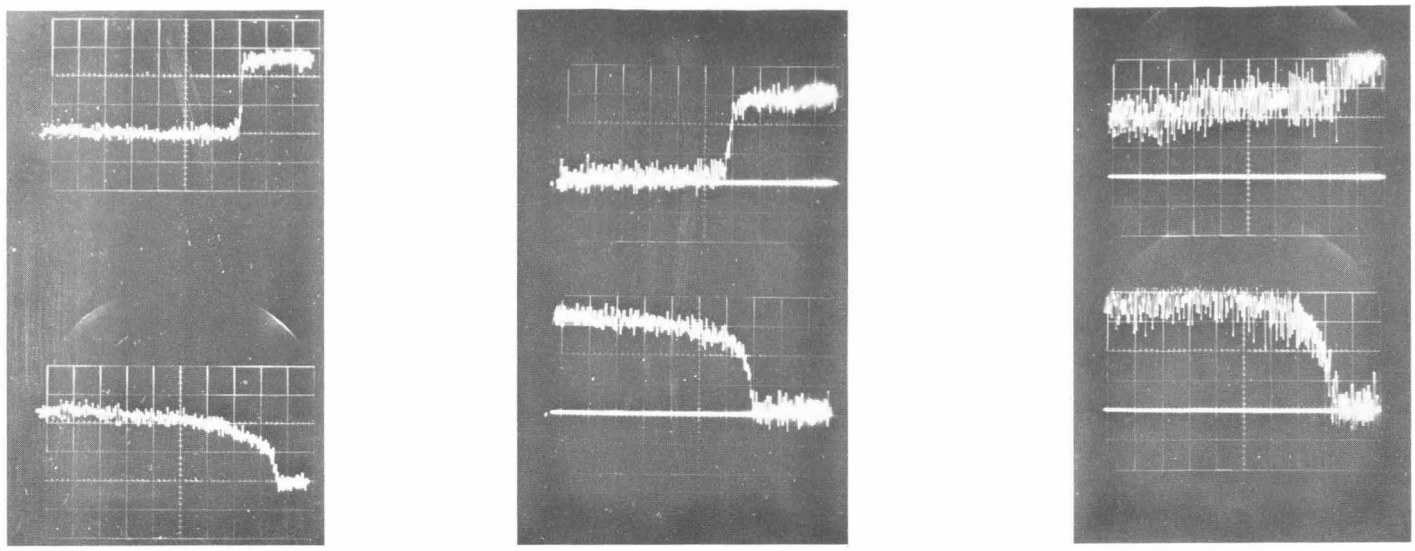

(a) (b) (c)

Fig. 11 - Oscilloscope traces of the force response. The upper trace shows the decay of the lift force when the ventilation supply is terminated. The lower shows the build-up of the force as ventilation commences. (a) is for a single port, (b) is for the nine-hole ventilation configuration (No. 4), (c) same as (a) except that the tunnel speed is 11 ft/sec. The time scale is 0.2 seconds per major division and the tunnel speed is 18.5 feet per second. Time increases to the left.

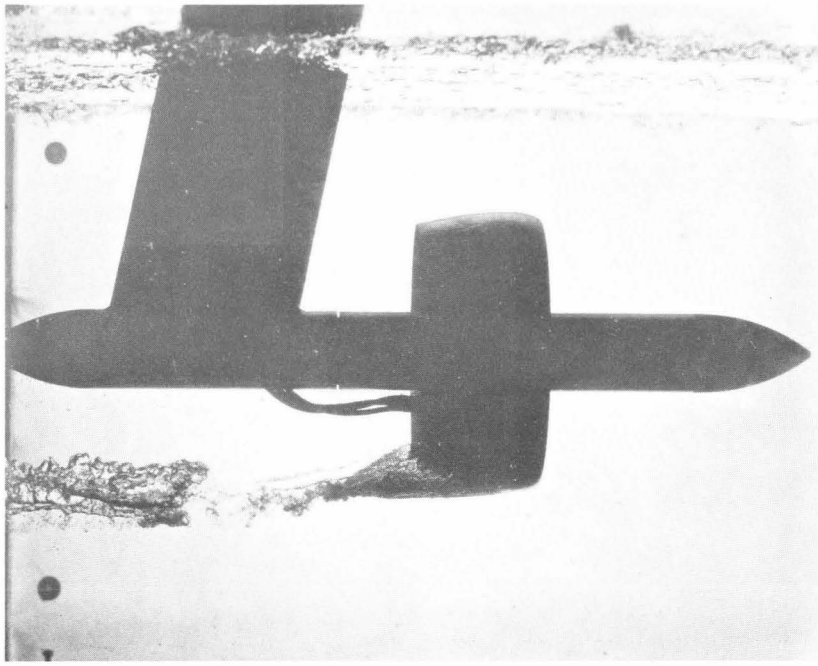

(a)

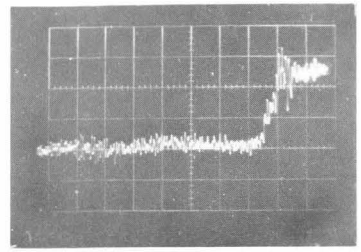

(c)

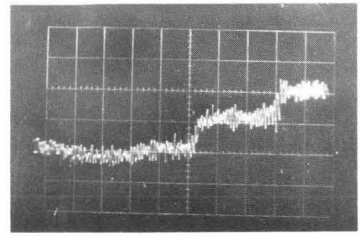

(b)

Fig. 12 - Photograph (a) and force traces (b) and (c) showing incomplete cavity break-off in the absence of a trip wire when the ventilation supply is terminated. A single ventilation hole is used. The time scale on the oscilloscope traces is 0.2 seconds per major division.

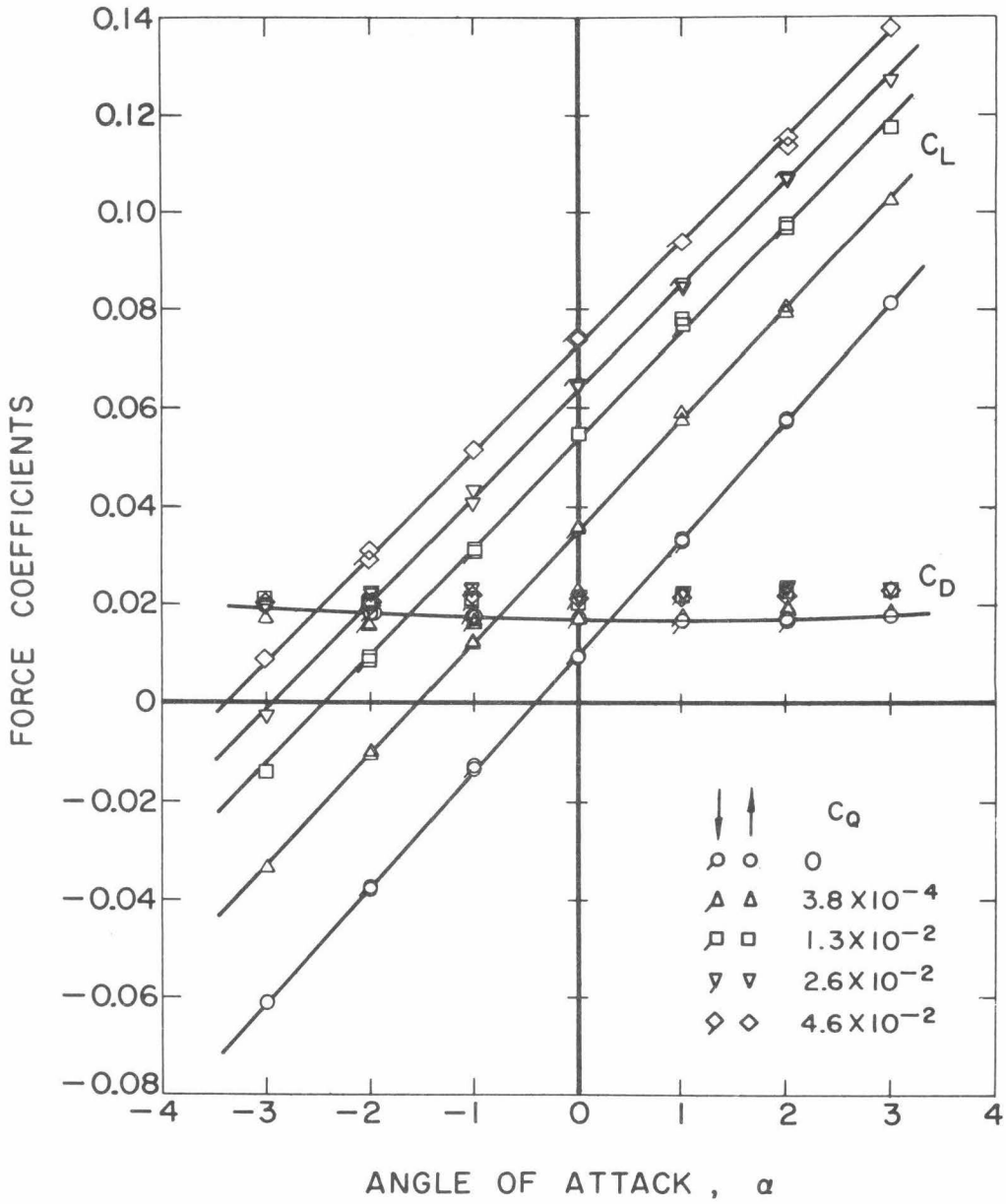

Fig. 13 - Force coefficients versus angle of attack with various air flow coefficients for the ring wing at a speed of 11 feet per second ($Re = 3.6 \times 10^5$) for ventilation hole configuration No. 5.

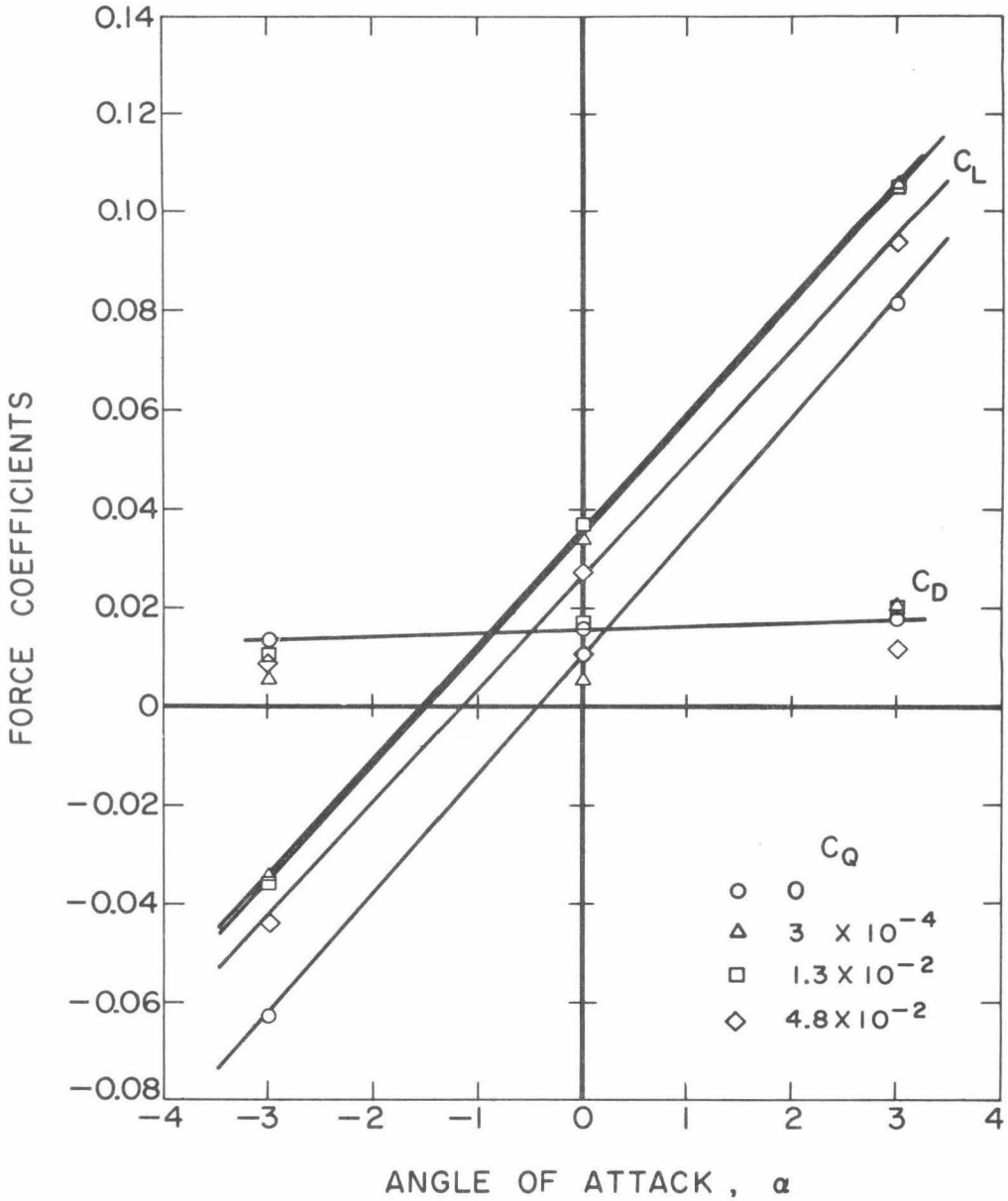

Fig. 14 - Force coefficients versus angle of attack with various air flow coefficients for the ring wing at a speed of 11 feet per second (Re = 3.6×10^5) for ventilation hole configuration No. 6.

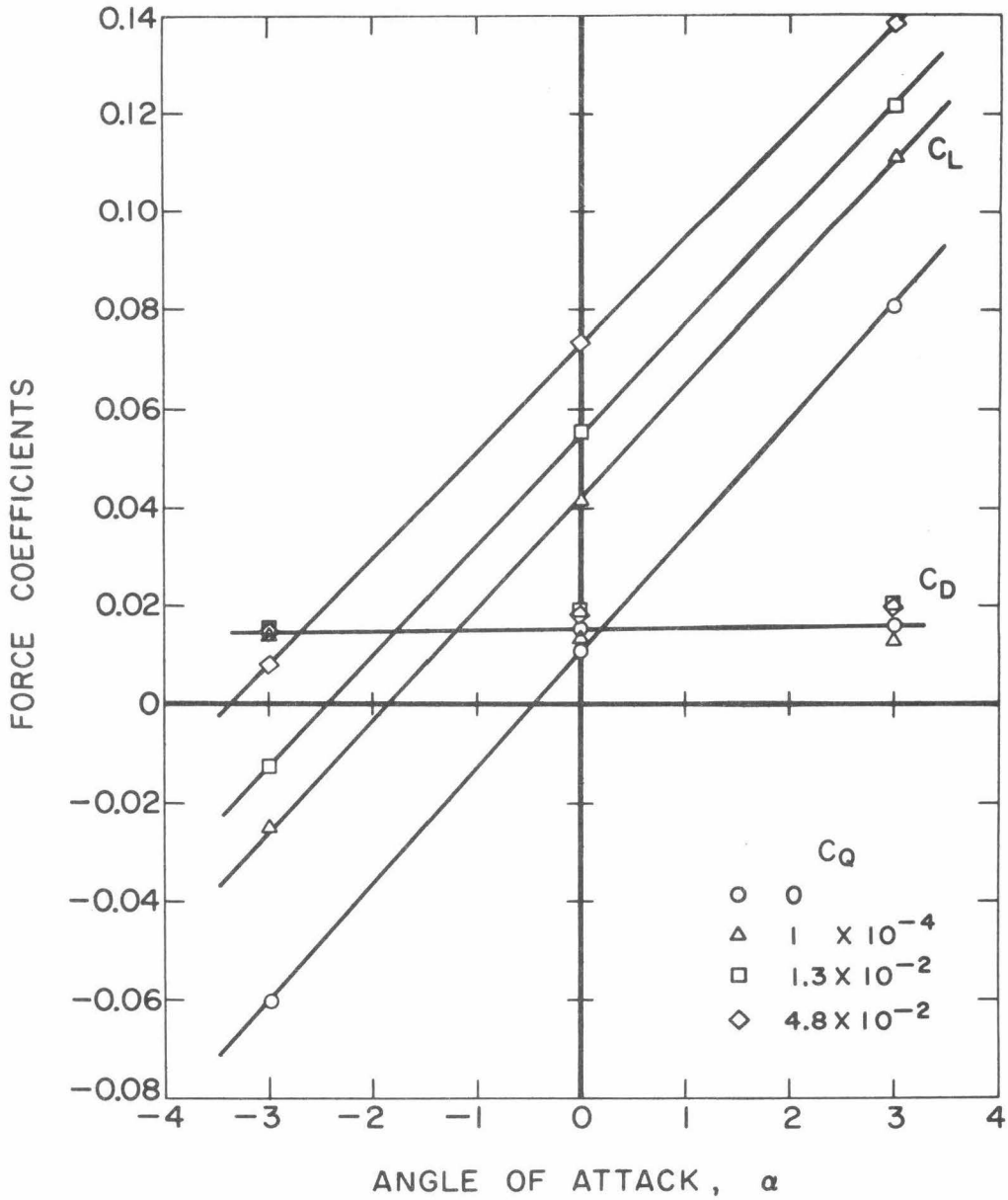

Fig. 15 - Force coefficients versus angle of attack with various air flow coefficients for the ring wing at a speed of 11 feet per second (Re = 3.6×10^5) for ventilation hole configuration No. 7.

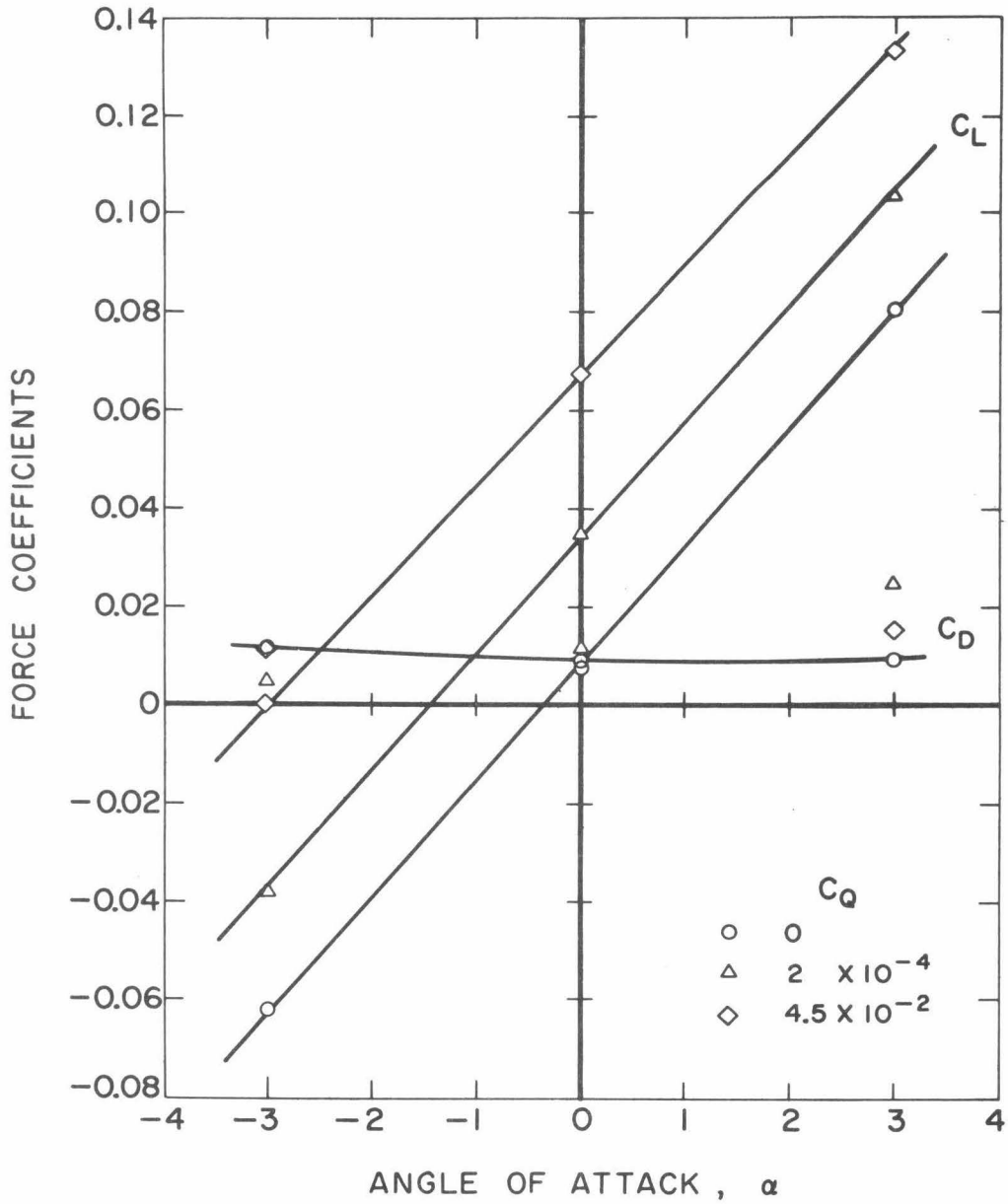

Fig. 16 - Force coefficients versus angle of attack with various air flow coefficients for the ring wing at a speed of 11 feet per second (Re = 3.6×10^5) for ventilation hole configuration No. 8.

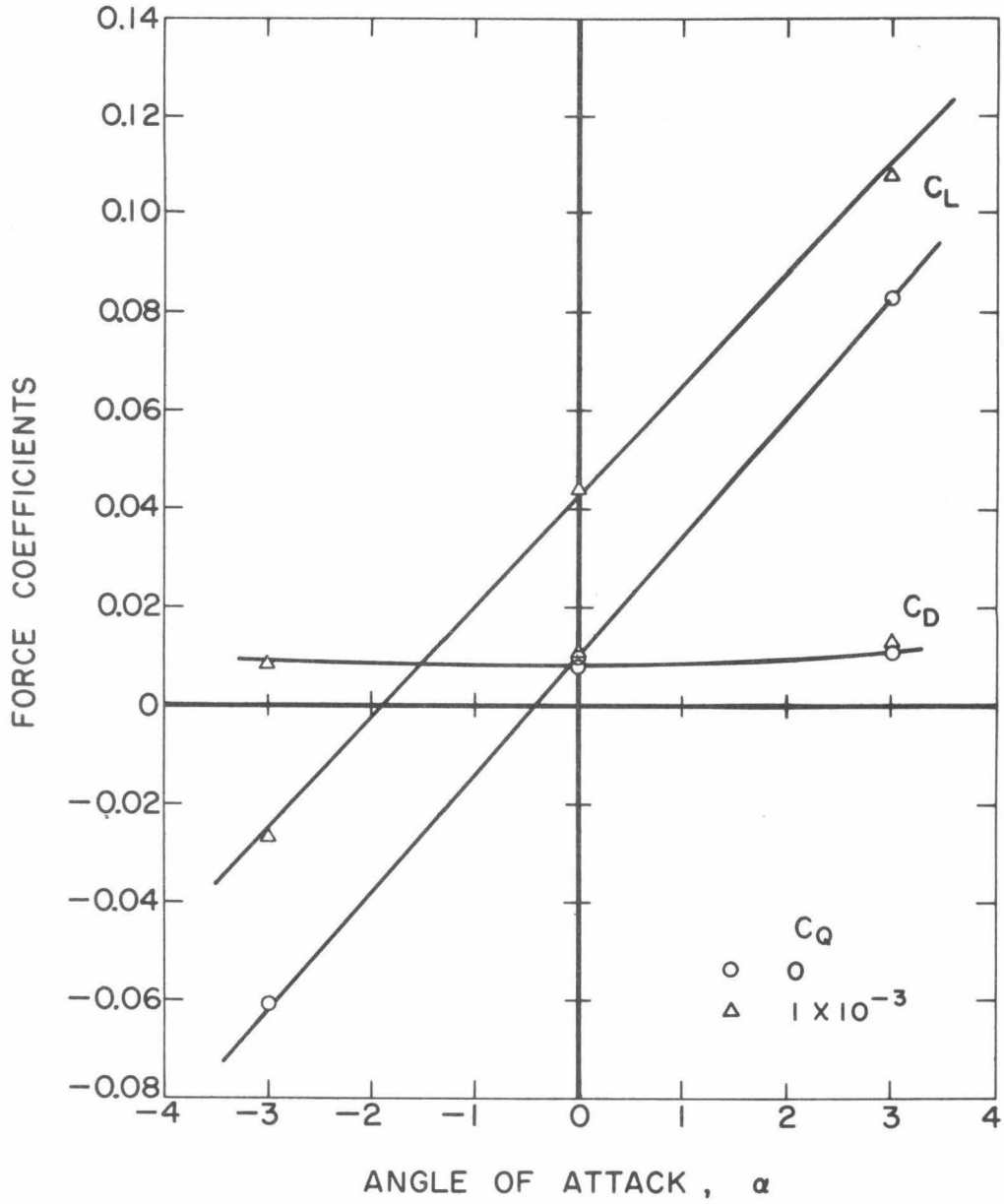

Fig. 17 - Force coefficients versus angle of attack with various air flow coefficients for the ring wing at a speed of 11 feet per second (Re = 3.6×10^5) for ventilation hole configuration No. 9.

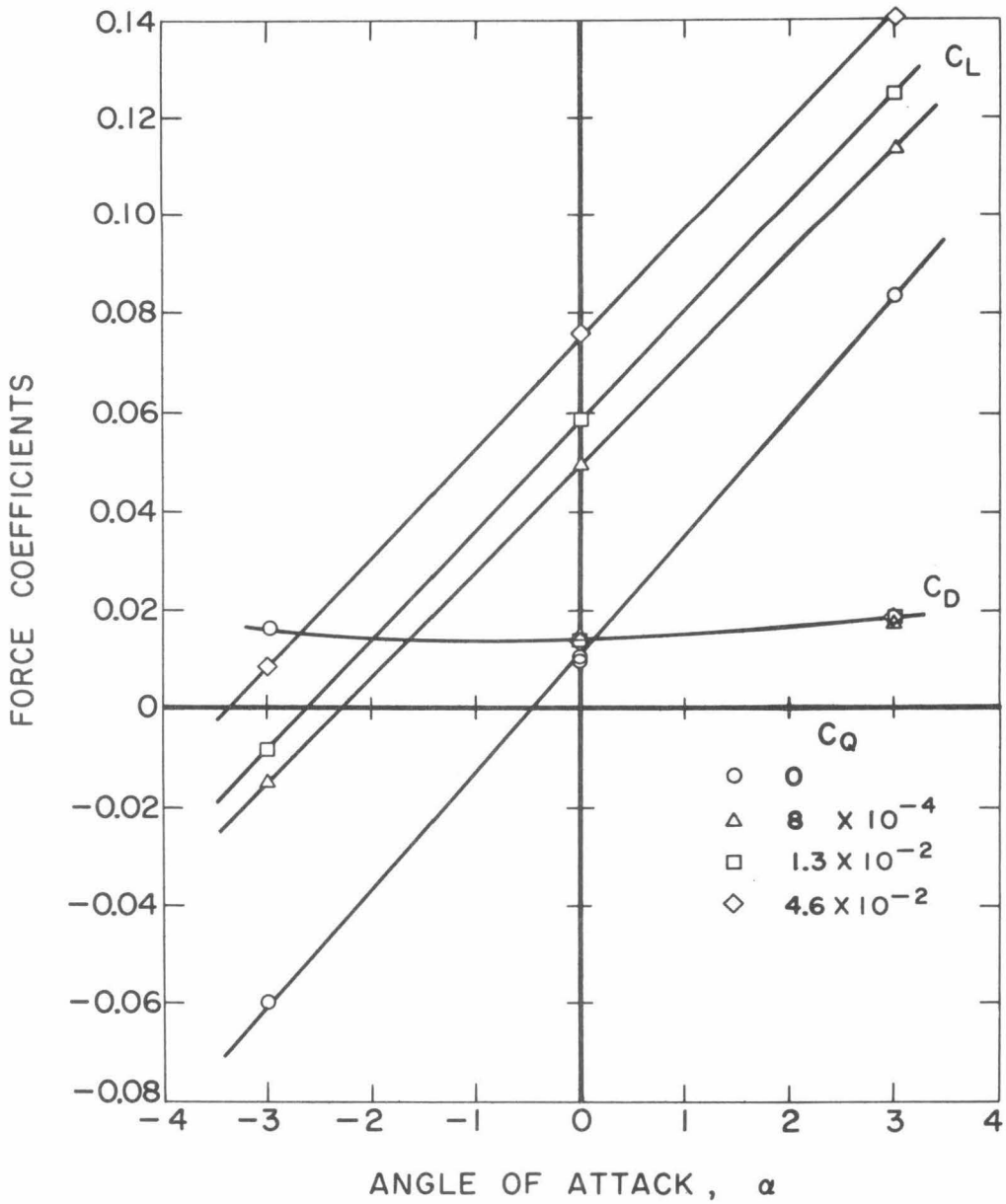

Fig. 18 - Force coefficients versus angle of attack with various air flow coefficients for the ring wing at a speed of 11 feet per second (Re = 3.6 x 10^5) for ventilation hole configuration No. 10.

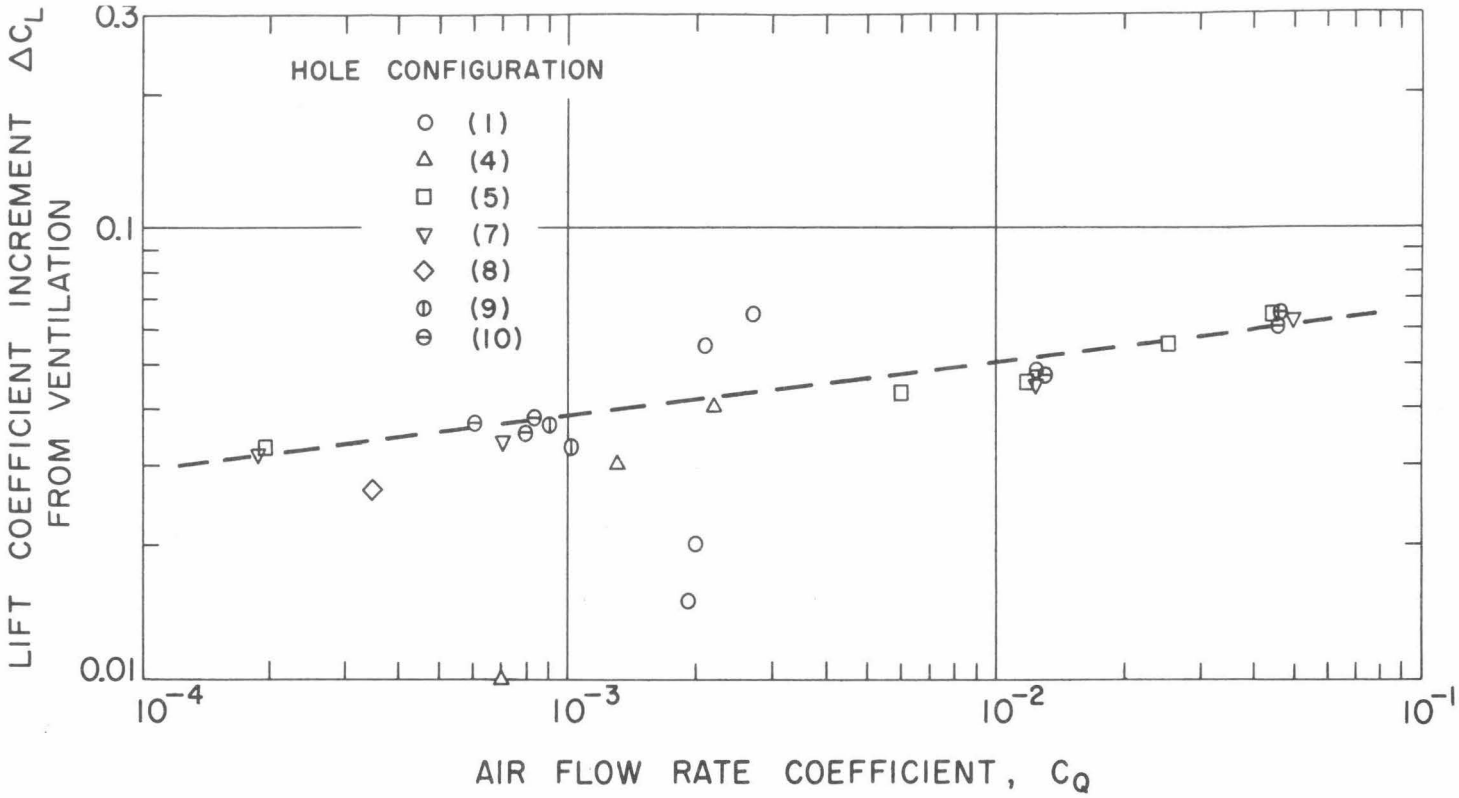

Fig. 19 - The effect of air flow rate coefficient, C_Q, on the lift increment for selective ventilation for various ventilation hole configurations.

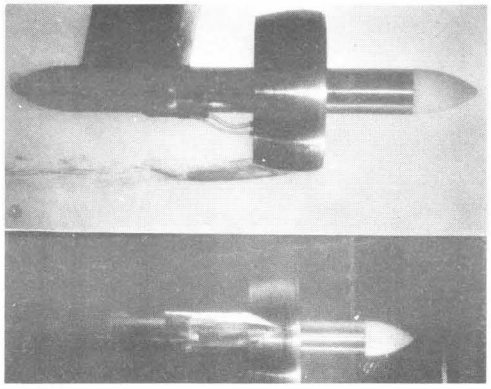

(a) $C_Q = 4.1 \times 10^{-4}$

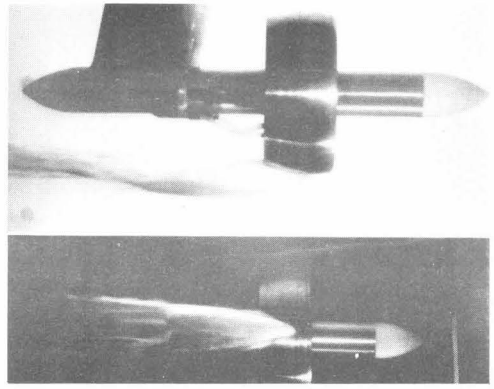

(a) $C_Q = 1.3 \times 10^{-2}$

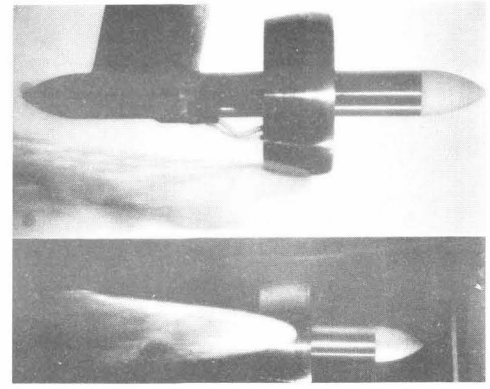

(a) $C_Q = 2.5 \times 10^{-2}$

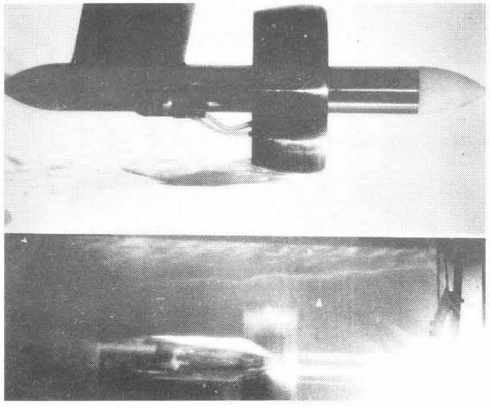

(b) $C_Q = 1.9 \times 10^{-4}$

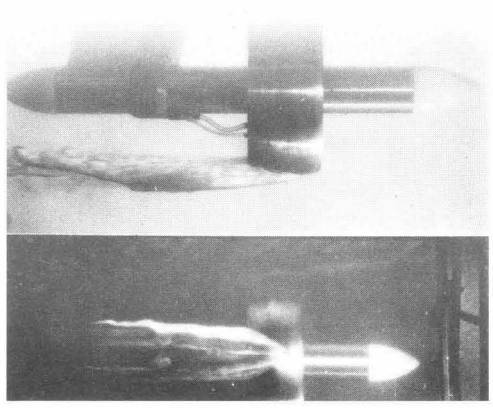

(b) $C_Q = 1.3 \times 10^{-2}$

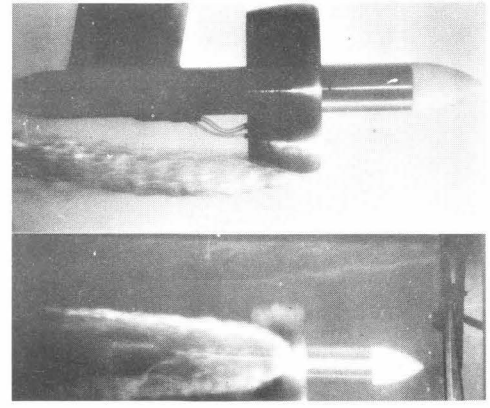

(b) $C_Q = 4.6 \times 10^{-2}$

Fig. 20 - Photographs of the ventilation cavity at zero angle of attack and various air flow coefficients on (a) ventilation hole configuration No. 5 (single hole), and (b) hole configuration No. 7 (cut-away deflector).

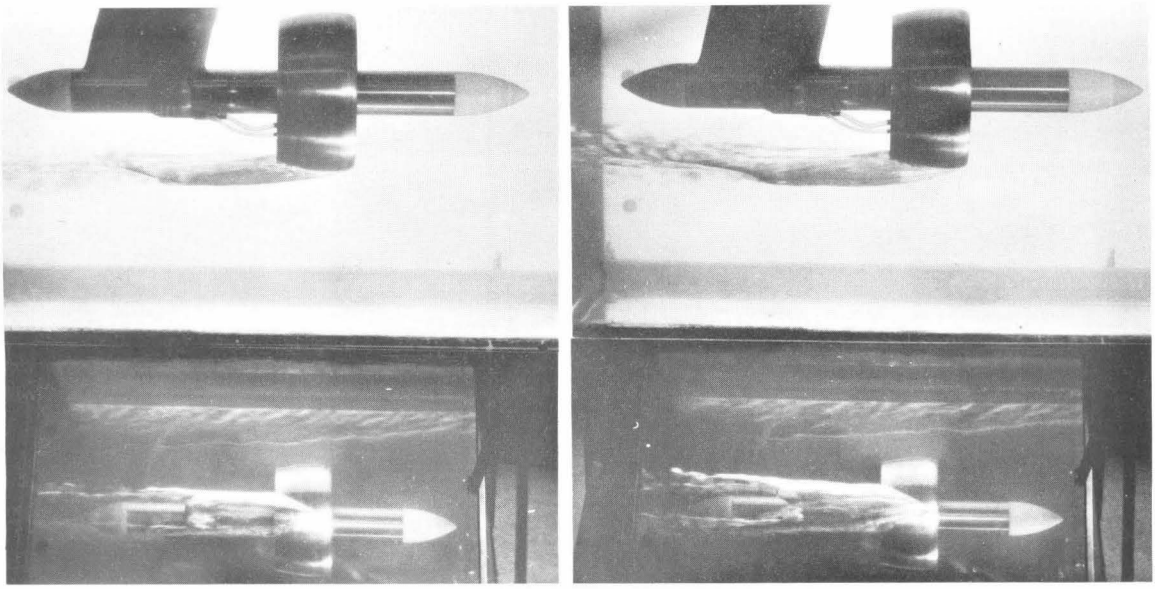

$C_Q = 8 \times 10^{-4}$

$C_Q = 1.3 \times 10^{-2}$

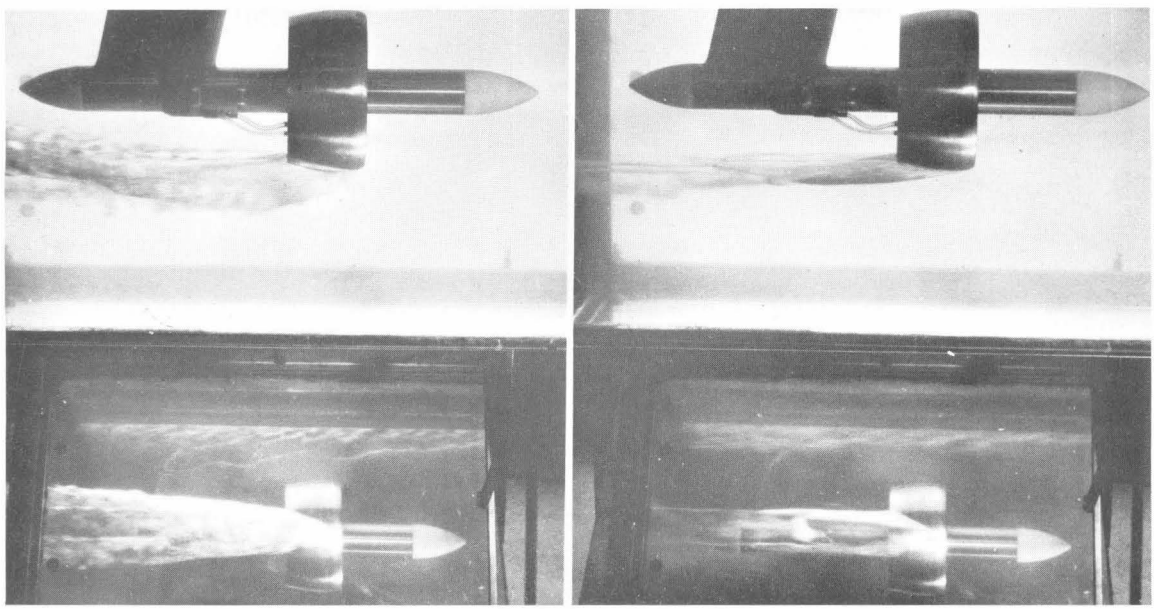

$C_Q = 4.6 \times 10^{-2}$

$C_Q = 6 \times 10^{-4}$

$V = 22$ ft/sec

Fig. 20 - (Concl.) Photographs of the ventilation cavity at zero angle of attack and various air flow rate coefficients on (c) ventilation hole configuration No. 10 (nine 1/16 inch holes). All photographs unless otherwise mentioned were taken at a tunnel speed of 11 feet per second.

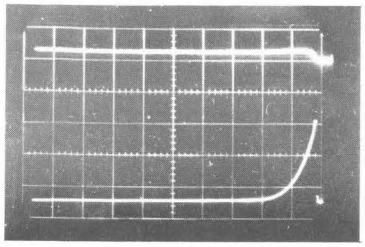

$C_Q = 1.9 \times 10^{-4}$

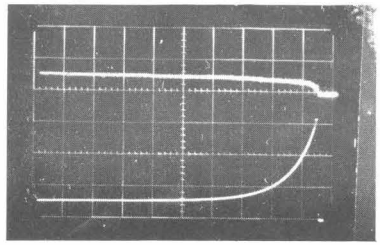

$C_Q = 1.2 \times 10^{-2}$

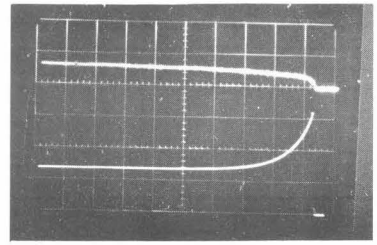

$C_Q = 2.5 \times 10^{-2}$

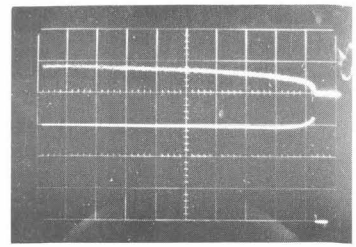

$C_Q = 4.6 \times 10^{-2}$

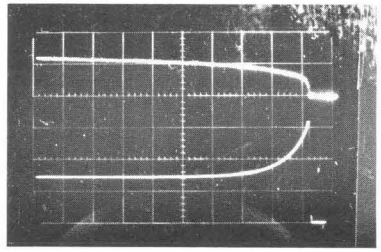

$C_Q = 0.7 \times 10^{-2}$
V = 22 ft/sec

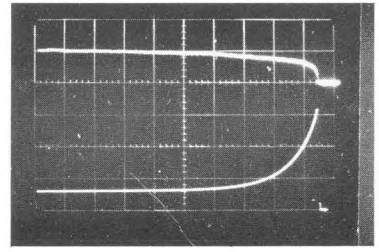

$C_Q = 1.3 \times 10^{-2}$
V = 22 ft/sec

Fig. 21(a) - Force time traces for zero angle of attack with hole configuration No. 5. Unless indicated, the tunnel speed is 11 ft/sec. The upper trace is the force and the lower trace is the supply pressure. The major time division is 0.5 seconds and time increases to the left.

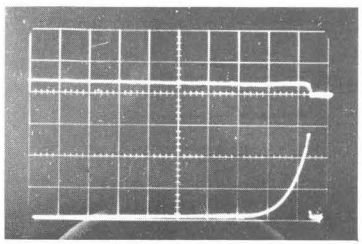

$C_Q = 1.9 \times 10^{-4}$

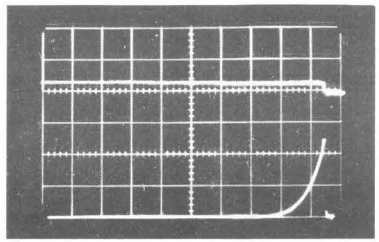

$C_Q = 3.3 \times 10^{-4}$

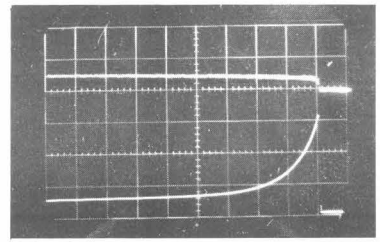

$C_Q = 1.3 \times 10^{-2}$

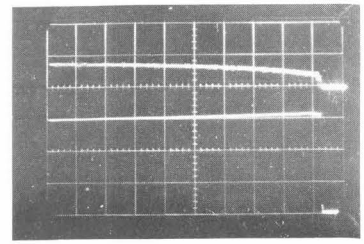

$C_Q = 4.6 \times 10^{-2}$

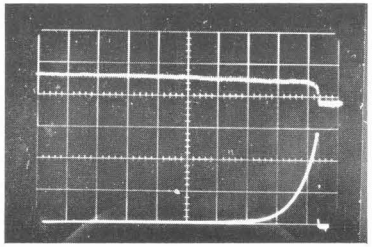

$C_Q = 7 \times 10^{-4}$
V = 22 ft/sec

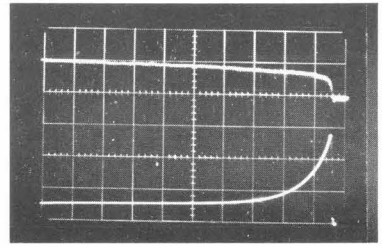

$C_Q = .6 \times 10^{-2}$
V = 22 ft/sec

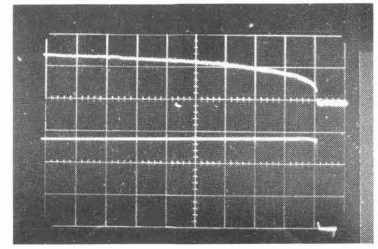

$C_Q = 2.2 \times 10^{-2}$
V = 22 ft/sec

Fig. 21(b) - Force time traces for zero angle of attack with hole configuration No. 7. Unless indicated, the tunnel speed is 11 ft/sec. The upper trace is the force and the lower trace is the supply pressure. The major time division is 0.5 seconds.

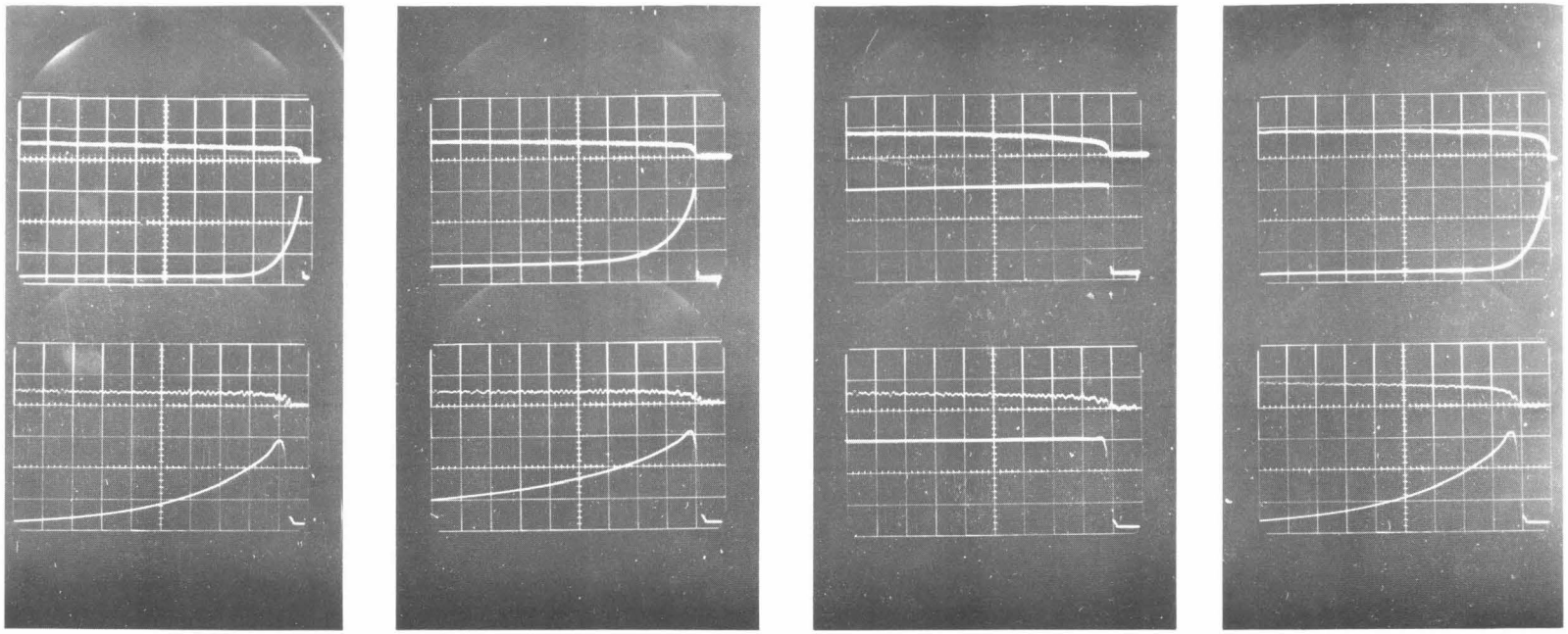

Fig. 21(c) - Force time traces for zero angle of attack with hole configuration No. 10. Unless indicated, the tunnel speed is 11 ft/sec. As in (b) and (c) the upper portion of each trace is the force and the lower part is the pressure. The upper diagram has a time scale of 0.5 seconds per major division and the lower diagram of each pair has a scale of 0.1 seconds per major division. The time histories for configurations 8 and 9 are similar.

APPENDIX

APPENDIX

TABLE A-1 - Dimensionless Coordinates Used for 10 Percent Clark Y Ring Airfoil

x/c	y/c_{upper}	y/c_{lower}	x/c	y/c_{upper}	y/c_{lower}
0	.0299	.0299	.350	.0995	0
.001	.0344	.0252	.400	.0974	0
.002	.0364	.0232	.450	.0940	0
.003	.0377	.0221	.475	.0920	0
.004	.0387	.0212	.500	.0899	0
.006	.0408	.0196	.525	.0872	0
.008	.0427	.0185	.550	.0845	0
.010	.0444	.0175	.575	.0817	0
.015	.0485	.0155	.600	.0782	0
.020	.0519	.0138	.625	.0750	0
.025	.0553	.0125	.650	.0710	0
.030	.0580	.0114	.675	.0670	0
.040	.0632	.0095	.700	.0628	0
.050	.0674	.0079	.725	.0582	0
.070*	.0741	.0057	.750	.0540	0
.090	.0797	.0042	.775	.0496	0
.110	.0843	.0030	.800	.0446	0
.130	.0881	.0020	.825	.0395	0**
.150	.0914	.0013	.850	.0342	0
.170	.0940	.0010	.875	.0295**	0
.190	.0964	.0006	.900	.0244	0
.210	.0980	.0003	.925	.0190	0
.230	.0988	.0001	.950	.0140	0
.250	.0994	.0001	.975	.0089	0
.300	.1000	0	1.000	.0030	0

Leading edge radius = 0.0109c.

*Approximate location of trip wire (diameter = 0.0025c)

**Denotes that all subsequent points have been slightly modified for fabrication

APPENDIX

TABLE A-2

VENT HOLE CONFIGURATIONS

Designation	Description
1	Three 1/32 inch holes spaced at one inch around circumference
2	Nine 1/32 inch holes spaced at 1/8 inch around circumference
3	Five 1/32 inch holes spaced at 1/8 inch around circumference
4	Three 1/32 inch holes spaced at 1/8 inch around circumference
5	Single hole (1/8 x 3/6 inch)
6	No. 5 with deflector
7	No. 5 with cut-away deflector
8	Six 1/16 inch holes
9	Eight 1/16 inch holes
10	Nine 1/16 inch holes

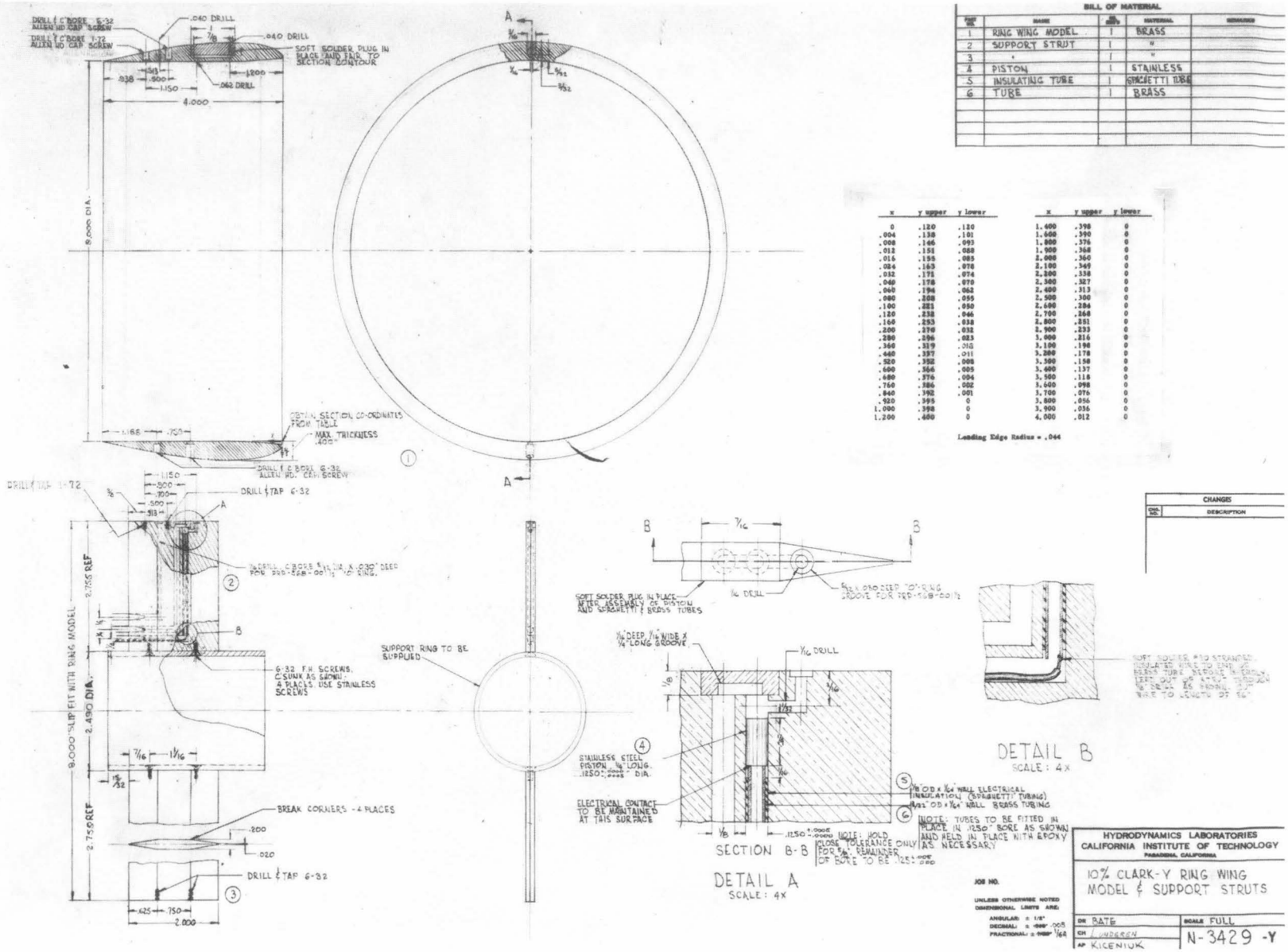

Fig. A-1 Ring Wing and Strut Support Assembly

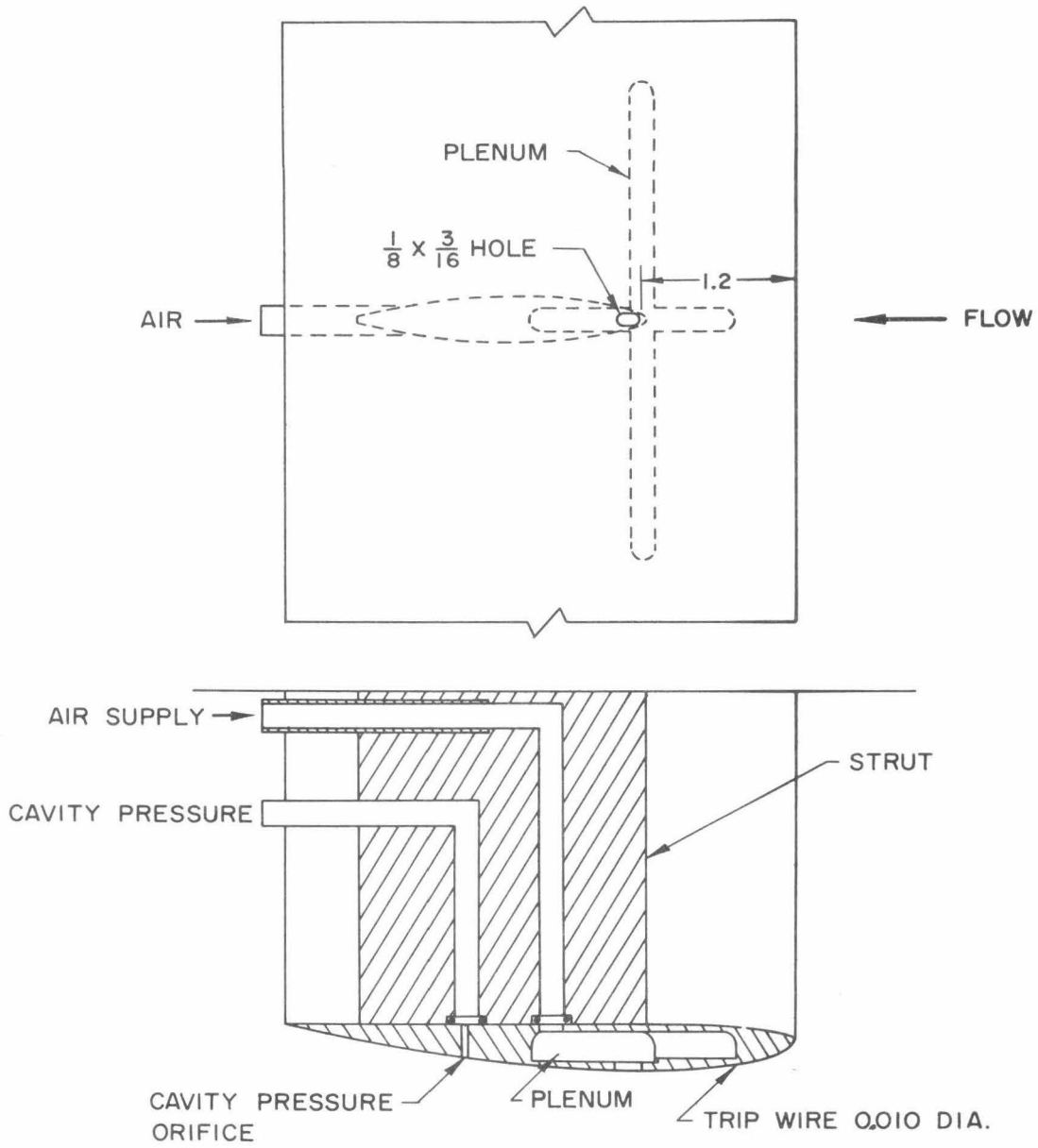

Fig. A-2 Schematic diagram showing hole configuration No. 5 and outline of plenum chamber for hole configurations No. 1 - 4.

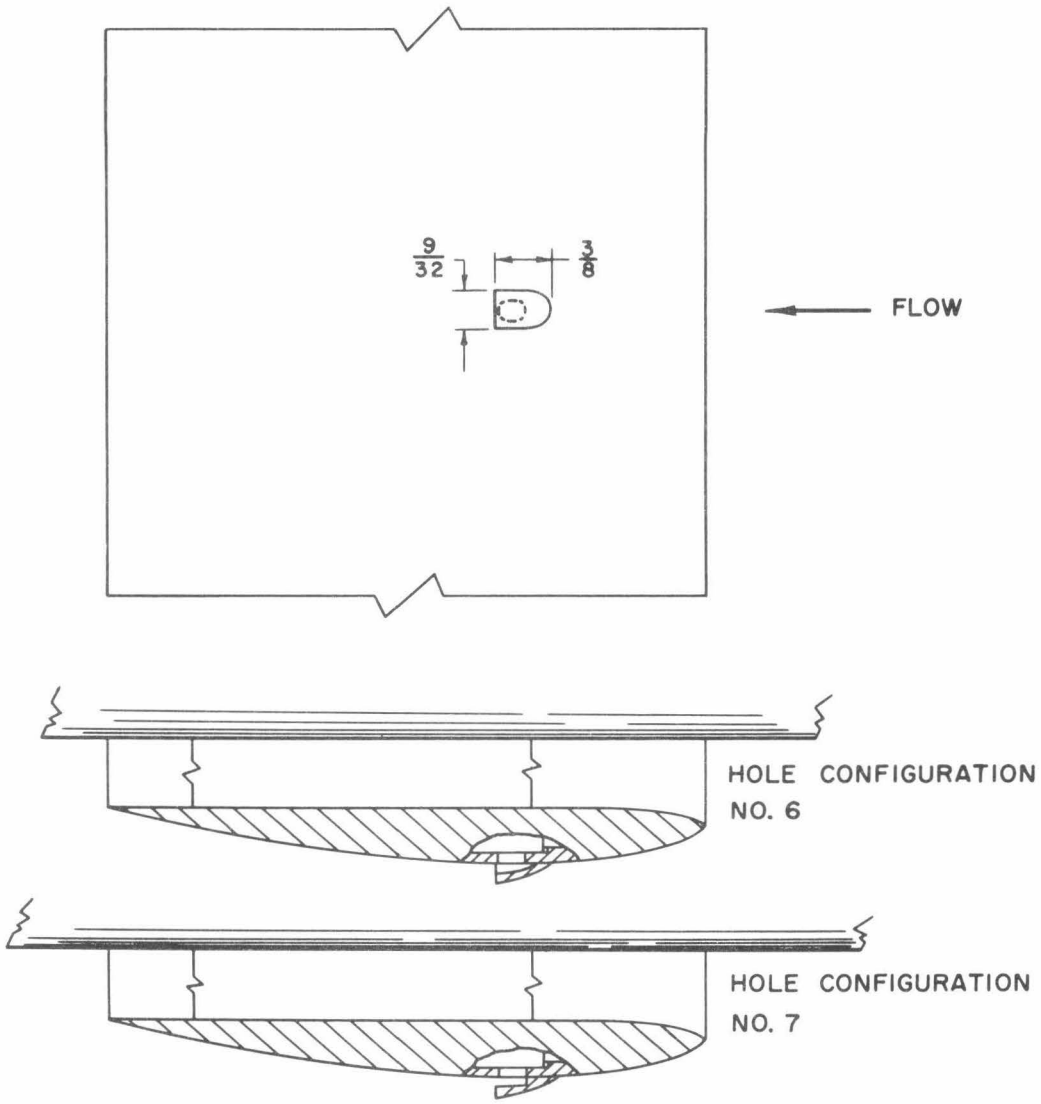

Fig. A-3 Schematic diagram of hole configurations Nos. 6 and 7 showing plenum chamber.

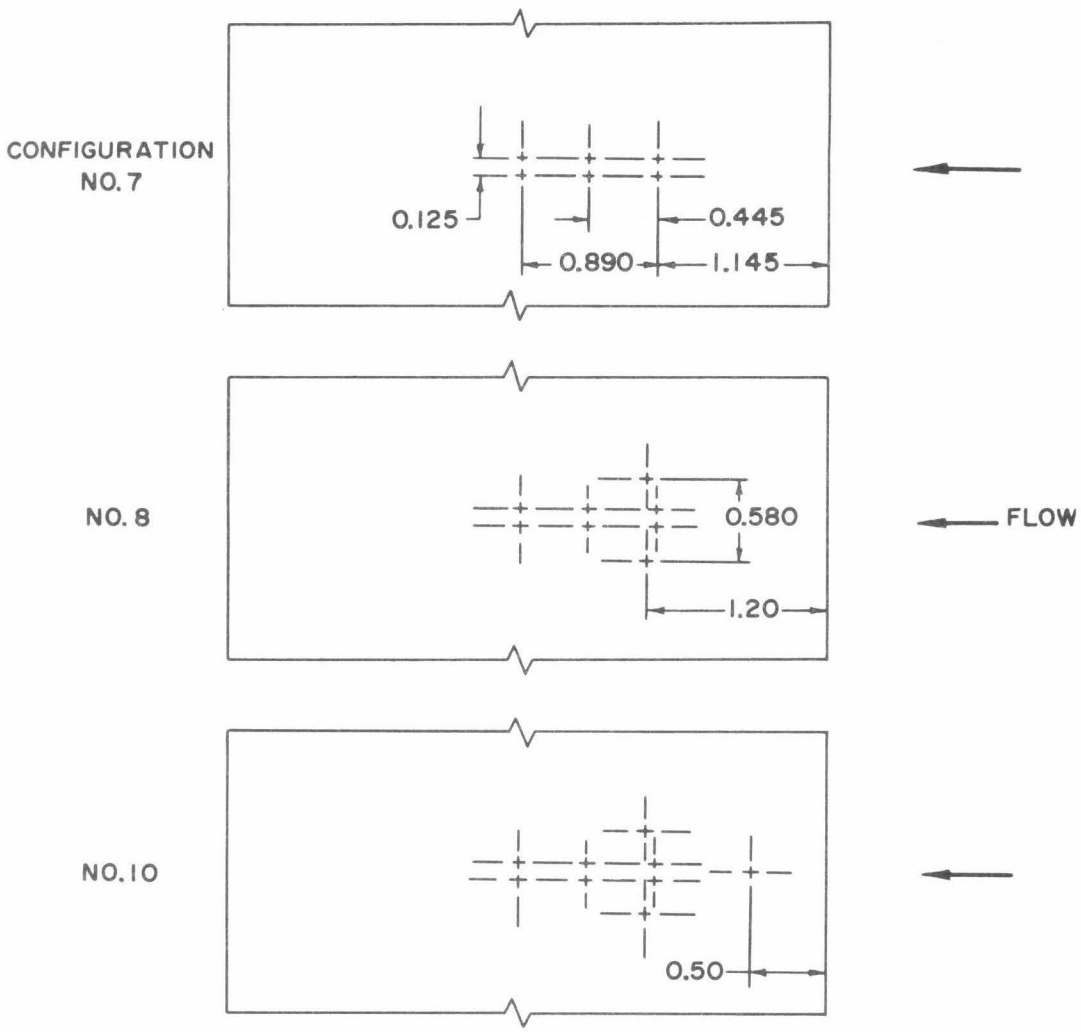

Fig. A-4 Hole configurations 7 - 10.

DISTRIBUTION LIST

Agency	Copies
Commander, Naval Ordnance Systems Command Department of the Navy, Washington, D.C. 20360	
Attn: Code ORD-035	2
Code ORD-0523	1
Code ORD-05413	1
Code ORD-9132	2
Code NSP-001	1
Code ASW-2000	1
Commander, Naval Air Systems Command Department of the Navy, Washington, D.C. 20360	
Attn: Code AIR-320	1
Commanding Officer and Director Naval Ship Research and Development Center Department of the Navy, Washington, D.C. 20007	
Attn: Code 500	1
Code 530	1
Commander, Naval Missile Center Point Mugu, California 93041	
Attn: Technical Library	1
Commander, Naval Weapons Center Inyokern, China Lake, California 93557	
Attn: Technical Library	1
Code 406	1
Commander, Naval Undersea Warfare Center Pasadena Annex, Pasadena, California 91107	
Attn: Code P-807	1
Code P-8552	1
Commander, Naval Ordnance Laboratory White Oak, Silver Spring, Maryland 20910	
Attn: Code 730	1
Code 530	1
Code 320	1
Commanding Officer, Naval Underwater Weapons Research & Engineering Station, Newport, Rhode Island 02844	
Attn: Code RE	1
Commanding Officer and Director, Naval Electronics Laboratory San Diego, California 92152	1
Commanding Officer, Naval Torpedo Station, Keyport, Wash. 98345	
Attn: Technical Library	1
Chief of Naval Research, Department of the Navy Washington, D.C. 20360	
Attn: Code 438	1
Code 461	1
Code 466	1

Agency	Copies
Commander, Naval Ships Systems Command Department of the Navy, Washington, D.C. 20360	
Attn: Code 2052	1
Code 034	1
Code 6136	1
Code 6114	1
Commander, Naval Oceanographic Office Washington, D. C. 20390	
Attn: Marine Science Department	1
Superintendent, U.S. Naval Postgraduate School Monterey, California 93940	1
Superintendent, U.S. Naval Academy Annapolis, Maryland 21402	1
Commander, Office of Aerospace Research 1400 Wilson Boulevard, Arlington, Virginia 22029	1
Commanding General, Army Material Command Department of the Army, Washington, D. C. 20315	
Attn: Chief Engineer	1
National Aeronautics and Space Administration Washington, D. C. 20546	
Attn: Code UST	2
Director, National Bureau of Standards Washington, D. C. 20234	
Attn: Fluid Mechanics Section	1
National Science Foundation, Washington, D.C. 20550	1
Commander, Defense Documentation Center Cameron Station, Alexandria, Virginia 22314	16
Alden Hydraulic Laboratory, Worcester Polytechnic Institute Worcester, Massachusetts 01609	
Attn: L. J. Hooper	1
Stevens Institute of Technology, Castle Point Hoboken, New Jersey 07030	
Attn: A. Suarez	1
Ordnance Research Laboratory, Pennsylvania State Univ. State College, Pennsylvania 16801	
Attn: G. F. Wislicenus	1
Department of Naval Architecture & Marine Engineering Massachusetts Institute of Technology, Cambridge, Mass. 02138	
Attn: Library	1

Agency	Copies
Applied Physics Laboratory, University of Washington Seattle, Washington 98105 Attn: Library	1
Aerojet-General Co., Azusa, California 91702 Attn: J. Levy	1
Douglas Aircraft Company, Inc., Aircraft Division Long Beach, California 90808 Attn: A.M.O. Smith	1
Eastern Research Group, New York, N. Y. 10005	1
General Dynamics, Convair Division, San Diego, Calif. 92112	1
Grumman Aircraft Engineering Corporation Bethpage, Long Island, New York 11714 Attn: Research Department	1
Hydronautics, Inc., Laurel, Maryland 20810 Attn: P. Eisenberg	1
Applied Physics Laboratory, The Johns Hopkins University Silver Spring, Maryland 20910 Attn: Library	1
Underwater Launch Department Lockheed Missile and Space Division, Sunnyvale, Calif. 94088	1
Northrop Corporation, Norair Division Hawthorne, California 90250 Attn: R. L. Jones	1
North American Aviation, Downey, California 90241 Attn: E. R. Van Driest	1
Advanced Systems Engineering, Westinghouse Electric Corp. Sunnyvale, California 94086 Attn: Technical Library	1

UNCLASSIFIED

Security Classifica

DOCUMENT CONTROL DATA - R&D

(Security classification of title, body of abstract and indexing annotation must be entered when the overall report is classified)

1. ORIGINATING ACTIVITY *(Corporate author)*
California Institute of Technology
Pasadena, California 91109

2a. REPORT SECURITY CLASSIFICATION
Unclassified

2b. GROUP

3. REPORT TITLE
Selectively Ventilated Ring Wings

4. DESCRIPTIVE NOTES *(Type of report and inclusive dates)*
Final Technical Report

5. AUTHOR(S) *(Last name, first name, initial)*
Acosta, Allan J. and Wade, Richard B.

6. REPORT DATE	7a. TOTAL NO. OF PAGES	7b. NO. OF REFS
August 1967		10

8a. CONTRACT OR GRANT NO.	9a. ORIGINATOR'S REPORT NUMBER(S)
Contract Nonr 220(54)	E-138.2
b. PROJECT NO.	
c.	9b. OTHER REPORT NO(S) *(Any other numbers that may be assigned this report)*
d.	

10. AVAILABILITY/LIMITATION NOTICES
Qualified requesters may obtain copies of this report direct from Defense Documentation Center, Cameron Station, Alexandria, Virginia 22314

11. SUPPLEMENTARY NOTES	12. SPONSORING MILITARY ACTIVITY
	Office of Naval Research, as administered by Bureau of Naval Weapons, Department of the Navy

13. ABSTRACT

Experiments were made on a ring wing having a chord-diameter ratio of one-half with a profile section consisting of a 10 percent Clark Y airfoil. Measurements were made of the force characteristics of this ring wing in fully wetted flow for several Reynolds numbers and angles of attack; in fully wetted flow these observations agreed with similar previous results on fully wetted ring wings. A portion of the circumference of the ring was also ventilated by the controlled injection of air to provide a cross-force. The magnitude of this cross-force varies with extent of ventilation and with the rate of injection of air. With less than approximately 11 percent of the trailing edge of the wing so ventilated, the cross-force corresponds to the wing in fully wetted flow having an angle of attack of nearly three degrees. Experiments were also made on the rapidity with which this cross-force could be built up at the start of injection or terminated after the ventilation had been established. The termination of the cross-force is very quick and amounts to a time approximately required for the flow to travel a distance of a few wing chords. The build-up process on the other hand is considerably slower, and it appears to be a dynamic one but the scaling laws for this phenomenon are not yet established.

DD FORM 1 JAN 64 1473 *0101-807-6800*

UNCLASSIFIED

14. KEY WORDS	LINK A		LINK B		LINK C	
	ROLE	WT	ROLE	WT	ROLE	WT
Ring Wing						
Ventilation						

INSTRUCTIONS

1. ORIGINATING ACTIVITY: Enter the name and address of the contractor, subcontractor, grantee, Department of Defense activity or other organization *(corporate author)* issuing the report.

2*a*. REPORT SECURITY CLASSIFICATION: Enter the overall security classification of the report. Indicate whether "Restricted Data" is included. Marking is to be in accordance with appropriate security regulations.

2*b*. GROUP: Automatic downgrading is specified in DoD Directive 5200.10 and Armed Forces Industrial Manual. Enter the group number. Also, when applicable, show that optional markings have been used for Group 3 and Group 4 as authorized.

3. REPORT TITLE: Enter the complete report title in all capital letters. Titles in all cases should be unclassified. If a meaningful title cannot be selected without classification, show title classification in all capitals in parenthesis immediately following the title.

4. DESCRIPTIVE NOTES: If appropriate, enter the type of report, e.g., interim, progress, summary, annual, or final. Give the inclusive dates when a specific reporting period is covered.

5. AUTHOR(S): Enter the name(s) of author(s) as shown on or in the report. Enter last name, first name, middle initial. If military, show rank and branch of service. The name of the principal author is an absolute minimum requirement.

6. REPORT DATE: Enter the date of the report as day, month, year; or month, year. If more than one date appears on the report, use date of publication.

7*a*. TOTAL NUMBER OF PAGES: The total page count should follow normal pagination procedures, i.e., enter the number of pages containing information.

7*b*. NUMBER OF REFERENCES: Enter the total number of references cited in the report.

8*a*. CONTRACT OR GRANT NUMBER: If appropriate, enter the applicable number of the contract or grant under which the report was written.

8*b*, 8*c*, & 8*d*. PROJECT NUMBER: Enter the appropriate military department identification, such as project number, subproject number, system numbers, task number, etc.

9*a*. ORIGINATOR'S REPORT NUMBER(S): Enter the official report number by which the document will be identified and controlled by the originating activity. This number must be unique to this report.

9*b*. OTHER REPORT NUMBER(S): If the report has been assigned any other report numbers *(either by the originator or by the sponsor)*, also enter this number(s).

10. AVAILABILITY/LIMITATION NOTICES: Enter any limitations on further dissemination of the report, other than those imposed by security classification, using standard statements such as:

(1) "Qualified requesters may obtain copies of this report from DDC."

(2) "Foreign announcement and dissemination of this report by DDC is not authorized."

(3) "U. S. Government agencies may obtain copies of this report directly from DDC. Other qualified DDC users shall request through

_____."

(4) "U. S. military agencies may obtain copies of this report directly from DDC. Other qualified users shall request through

_____."

(5) "All distribution of this report is controlled. Qualified DDC users shall request through

_____."

If the report has been furnished to the Office of Technical Services, Department of Commerce, for sale to the public, indicate this fact and enter the price, if known.

11. SUPPLEMENTARY NOTES: Use for additional explanatory notes.

12. SPONSORING MILITARY ACTIVITY: Enter the name of the departmental project office or laboratory sponsoring *(paying for)* the research and development. Include address.

13. ABSTRACT: Enter an abstract giving a brief and factual summary of the document indicative of the report, even though it may also appear elsewhere in the body of the technical report. If additional space is required, a continuation sheet shall be attached.

It is highly desirable that the abstract of classified reports be unclassified. Each paragraph of the abstract shall end with an indication of the military security classification of the information in the paragraph, represented as *(TS)*, *(S)*, *(C)*, or *(U)*.

There is no limitation on the length of the abstract. However, the suggested length is from 150 to 225 words.

14. KEY WORDS: Key words are technically meaningful terms or short phrases that characterize a report and may be used as index entries for cataloging the report. Key words must be selected so that no security classification is required. Identifiers, such as equipment model designation, trade name, military project code name, geographic location, may be used as key words but will be followed by an indication of technical context. The assignment of links, roles, and weights is optional.